C,C´-Bis(benzodiazaborolyl)dicarba-*closo*-dodecaboranes: Synthesis, Structures, Photophysics and Electrochemistry

Lothar Weber,*[,a] Jan Kahlert,[a] Regina Brockhinke,[a] Lena Böhling,[a] Johannes Halama,[a] Andreas Brockhinke,[a] Hans-Georg Stammler,[a] Beate Neumann,[a] Carlo Nervi,[b] Rachel A. Harder[c] and Mark A. Fox[c]

[a] Fakultät für Chemie der Universität Bielefeld, 33615 Bielefeld, Germany

E-mail: lothar.weber@uni-bielefeld.de

[b] Dipartimento di Chimica IFM, via P. Giuria 7, 10125 Torino, Italy

[c] Department of Chemistry, Durham University, Durham DH1 3LE, United Kingdom

Abstract:

Six new C,C´-bis(benzodiazaborolyl)dicarba-*closo*-dodecaboranes, 1,A-R_2-1,A-$C_2B_{10}H_{10}$, where R represents the group 2-(1,3-Et_2-1,3,2-$N_2BC_6H_4$) or 2-(1,3-Ph_2-1,3,2-$N_2BC_6H_4$) and A is 2, 7 or 12, were synthesized from *o*-, *m*-, and *p*-dicarbadodecarboranes (carboranes) by lithiation and subsequent treatment with the respective 2-bromo-1,3,2-benzodiazaboroles. UV-visible and fluorescence spectra of all carboranes display low energy charge transfer emissions. While such emissions with Stokes shifts between 17330 and 21290 cm^{-1} are typical for C,C´-bis(aryl)-*ortho*-carboranes, the observed low-energy emissions with Stokes shifts between 8320 and 15170 cm^{-1} for the *meta*- and *para*-isomers are unusual as high-energy emissions are typical for *meta*- and *para*-dicarbadodecaboranes. Fluorescence quantum yields (ϕ_F) for the novel 1,7- and 1,12-bis(benzodiazaborolyl)-carbaboranes depend on the substituents at the nitrogen-atoms of the heterocycle. Thus, the *para*-carborane with *N*-ethyl substituents 1,12-(1´,3´-Et_2-1´,3´,2´-$N_2BC_6H_4$)$_2$-1,12-$C_2B_{10}H_{10}$ has a ϕ_F value of 41% in cyclohexane solution and only of 9% in the solid state, whereas the analogous 1,12-(1´,3´-Ph_2-1´,3´,2´-$N_2BC_6H_4$)$_2$-1,12-$C_2B_{10}H_{10}$ shows quantum yields of 3% in cyclohexane solution and 72% in the solid state. X-ray crystallographic, computational and cyclic voltammetry studies for these carboranes are also presented.

Introduction

Organic light-emitting diodes (OLEDs) are of great attraction worldwide due to their potential applications in full-colour displays and solid state lights. Small molecules with bipolar electron-transporting character are extremely desirable as they offer the possibility to achieve efficient and stable OLEDs even in a simple single-layer device.[1] Tremendous efforts have been devoted to the design of materials with comparable hole- and electron-transporting abilities (such as donor-acceptor molecules) which are also called ambipolar materials.[2] Luminescent molecules with entirely new donor and acceptor units are desirable in the quest for stable and efficient OLEDs.

Since their discovery five decades ago, an extensive and rich chemistry of the three icosahedral carboranes, *ortho*-, *meta*- and *para*-$C_2B_{10}H_{12}$ has been established.[3] These carboranes have only recently been considered as potential components for OLEDs in photophysical studies on C,C-diarylated dicarbadodecaboranes.[4-13] Selected photophysical data for some C,C-diarylcarboranes are summarized in Chart 1.[4-7]

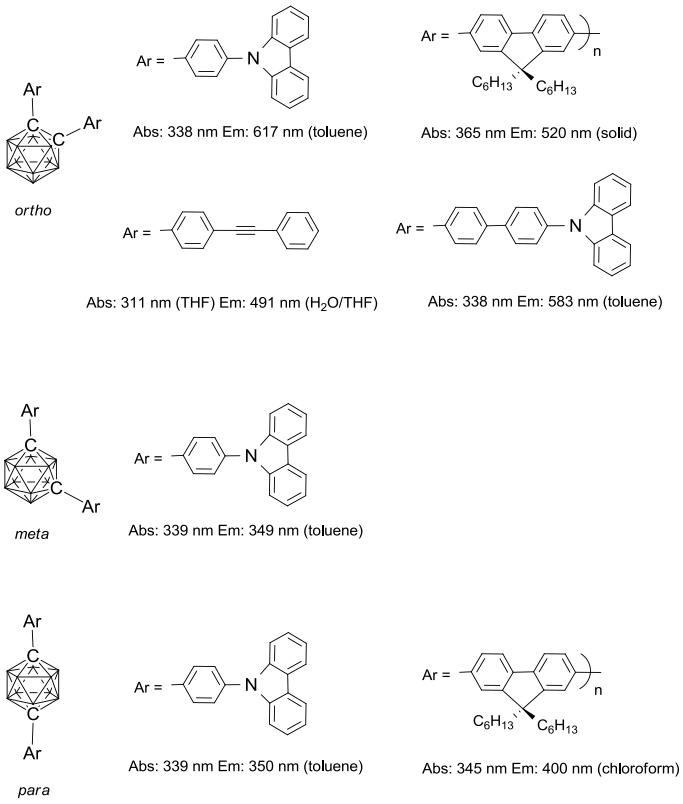

Chart 1.

The *meta*- and *para*-carborane clusters are generally considered as inductively electron-withdrawing pseudo-aromatic spacers with subtle effects on the emission spectra of

these fluorophors.[4,7,9-19] Due to similarities in their sizes, the *para*-carborane motif -$CB_{10}H_{10}C$- has been compared with the *para*-phenylene spacer 1,4-C_6H_4- in donor-acceptor molecules. There, however, the carborane behaved as an effective insulator, whereas the phenylene-moiety is well known as an electron-conducting conjugated π-system.[14] The *ortho*-carborane cluster, on the other hand, is a more powerful electron-withdrawing unit with a remarkably flexible C-C bond within the cage.[15] These features give rise to differerent photophysical behaviour of fluorophors with *ortho*-carborane building blocks, where in the solid state low-energy charge transfer emissions frequently occurred upon UV irradiation.[4,6,8,12] The cluster geometries of the excited states are presumably similar to the structures of carborane radical anions, where the cage C-C bond is significantly elongated by accommodation of the extra electron.[16,17] Carborane containing OLEDs were first reported in 2012 as polymer-light emitting diodes (PLEDs based on *ortho*-carborane with Ar=fluorene polymer, Chart 1)[18] and phosphorescent organic light emitting diodes (PHOLEDs based on *ortho*-, *meta*- and *para*-carboranes with Ar=carbazolyl; Chart 1).[19]

In the past decade, the chemistry of 1,3,2-benzodiazaboroles has seen a rapid development.[8,17,20-24] OLEDs fabricated from iridium and platinum chromophors with benzodiazaborolyl ligands emit blue or green light.[25] However, efficient and long-standing OLEDs from fluorescent organic molecules[20-23] and polymers[26] containing benzodiazaborole functions have not been reported to date.

We recently described the synthesis and photophysical behaviour of a series of *ortho* carboranes (**1**-**15**, Chart 2) featuring a 1,3-diethyl-, 1,3-diisopropyl-, 1,3-diphenyl- or 1,3-dihydro-1,3,2-benzodiazaborolyl substituent at one cage carbon atom.[8,17] Apart from **6** and **10**, these compounds show remarkable low-energy fluorescence emissions with Stokes shifts of 15100-20260 cm^{-1} and quantum yields up to 70% in the solid state. These low-energy emissions are due to a charge transfer between the electron-accepting cage and the electron-donating benzodiazaborolyl unit. These are luminescent molecules with a fundamentally new combination of donor- and acceptor functionalities which are of potential use in the fabrication of efficient solid state OLEDs. In view of these results, it was logical to explore *meta*- and *para*-carborane benzodiazaboroles in order to evaluate the influence of different cluster isomers on their photophysical properties.

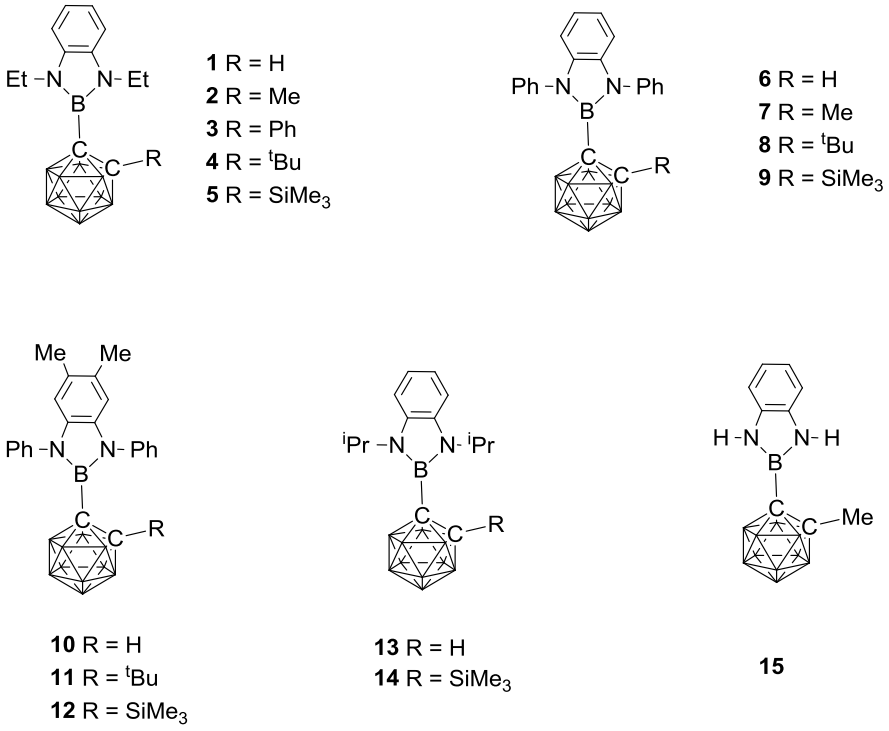

Chart 2.

Here we describe the synthesis, structural, photophysical and quantum-chemical studies for the six novel *ortho*-, *meta*- and *para*-carboranes **16**-**21** (Chart 3) where each cluster carbon atom is ligated by a benzodiazaborolyl group. For comparison, 2-*tert*-butyl-1,3,2-benzodiazaboroles **22** and **23** are considered because of the similar steric requirements of the *tert*-butyl group and the carborane cage.

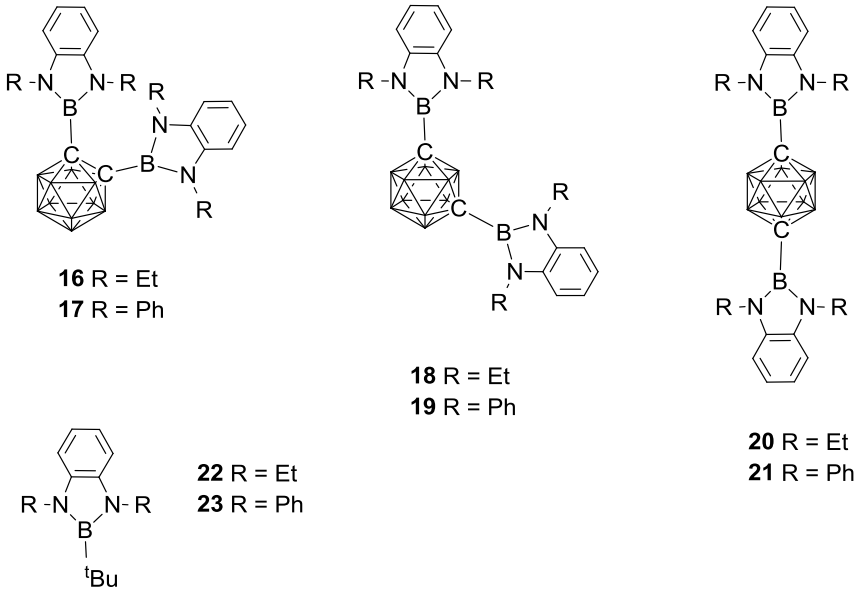

Chart 3.

Results and Discussion

Syntheses

Metallation of *ortho*-, *meta*- and *para*-carboranes with 2 equivalents of *n*-or *tert*-butyllithium and the subsequent treatment of the reaction mixtures with 2 equivalents of 2-bromo-1,3-diethyl-1,3,2-benzodiazaborole[31] or 2-bromo-1,3-diphenyl-1,3,2-benzodiazaborole,[23] respectively, afforded the bis(diazaborolyl)carboranes **16**-**21** (Scheme 1). The products were isolated by short-path distillation and purified by crystallisation (8-42% yield).

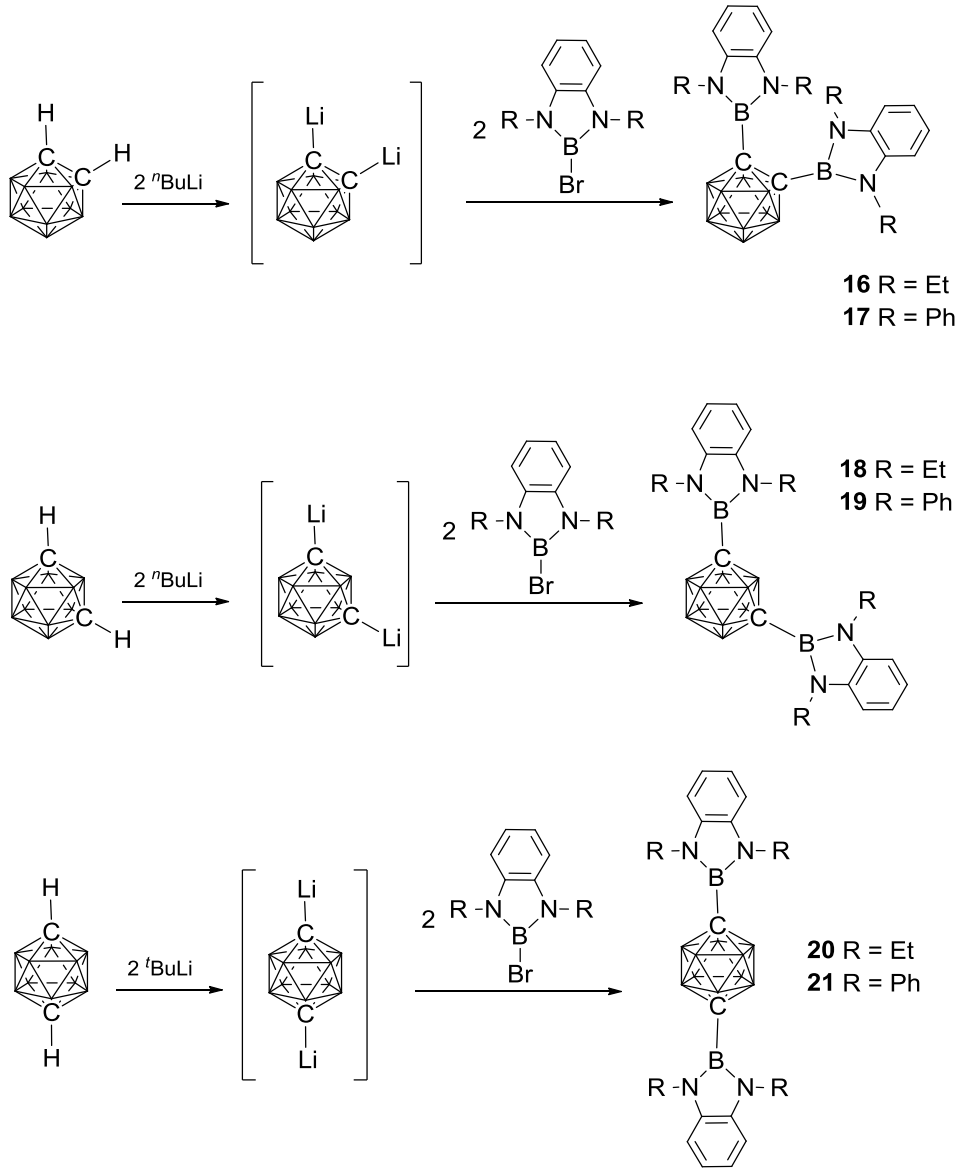

Scheme 1: General route to C,C´-bis(benzodiazaborolyl)carboranes **16**-**21**

The colourless compounds **16**-**21** are well soluble in dichloromethane, chloroform and aromatic hydrocarbons but only sparingly soluble in *n*-hexane. The solubility generally

decreases in order from *ortho*, *meta*- to *para*-carboranes. Solutions of the compounds are oxygen- and moisture sensitive. In the solid state, the 1,3-diphenyl-1,3,2-benzodiazaboroles **17**, **19** and **21** may be stored in air for days without visible deterioration.

In the ^{1}H NMR spectra of the 1,3-diethyl-1,3,2-benzodiazaboroles **16**, **18** and **20**, the peaks corresponding to the ethyl groups are found as quartets at δ = 3.57 - 4.00 ppm and triplets at δ = 0.92 - 1.34 ppm arising from $^{3}J_{HH}$ couplings. The NMR data for **16** suggest that there are no rotational barriers at the C1-B2' and C2-B2" bonds in solution for **16** so all rotational conformers probably exist in solution (for atom numbering see Figure 1).

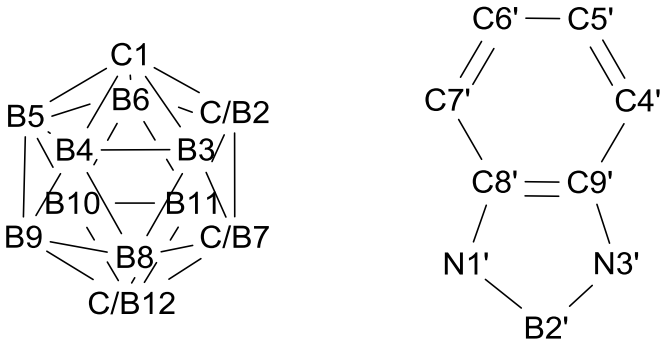

Figure 1. Numbering schemes used for the carborane cluster and the benzodiazaborolyl group. For discussion of the second benzodiazaborolyl group at C2, C7 or C12, the labels N1" for N1', B2" for B2' etc are used.

For the phenyl-substituted benzodiazaboroles, **19** and **21**, the ^{1}H NMR spectra display two apparent multiplets at δ = 7.15 (H_{ortho}) and δ = 7.44 ppm (H_{meta}, H_{para}) corresponding to the phenyl groups. By contrast, in the *ortho*-carborane **17**, five broad signals for the phenyl group hydrogens are recorded [δ = 5.90, 7.20 ppm (H_{ortho}, $H_{ortho'}$), δ = 6.98, 7.50 ppm (H_{meta}, $H_{meta'}$), δ = 7.36 ppm (H_{para})] (Figure S5). The ^{13}C{^{1}H} NMR spectrum of **17** also revealed two sets of resonances corresponding to the *ortho* and *meta* carbons of the phenyl groups (Figure S7). This is consistent with restricted intramolecular rotations around the C1-B2', C2-B2" and the four Ph-N bonds in **17**. It is thus likely that the rotations at the Ph-N bonds in the diphenylbenzodiazaborolyl groups are restricted in **19** and **21** as well. The shift difference of 1.3 ppm between the two *ortho*-phenyl proton peaks in **17** is remarkable and suggests that one set of protons is strongly shielded by π-electron fields from aryl groups in close proximity. The broad proton peaks were sharpened at -45°C (Figure 2) showing the two *ortho*-protons at 5.81 and 7.23 ppm.

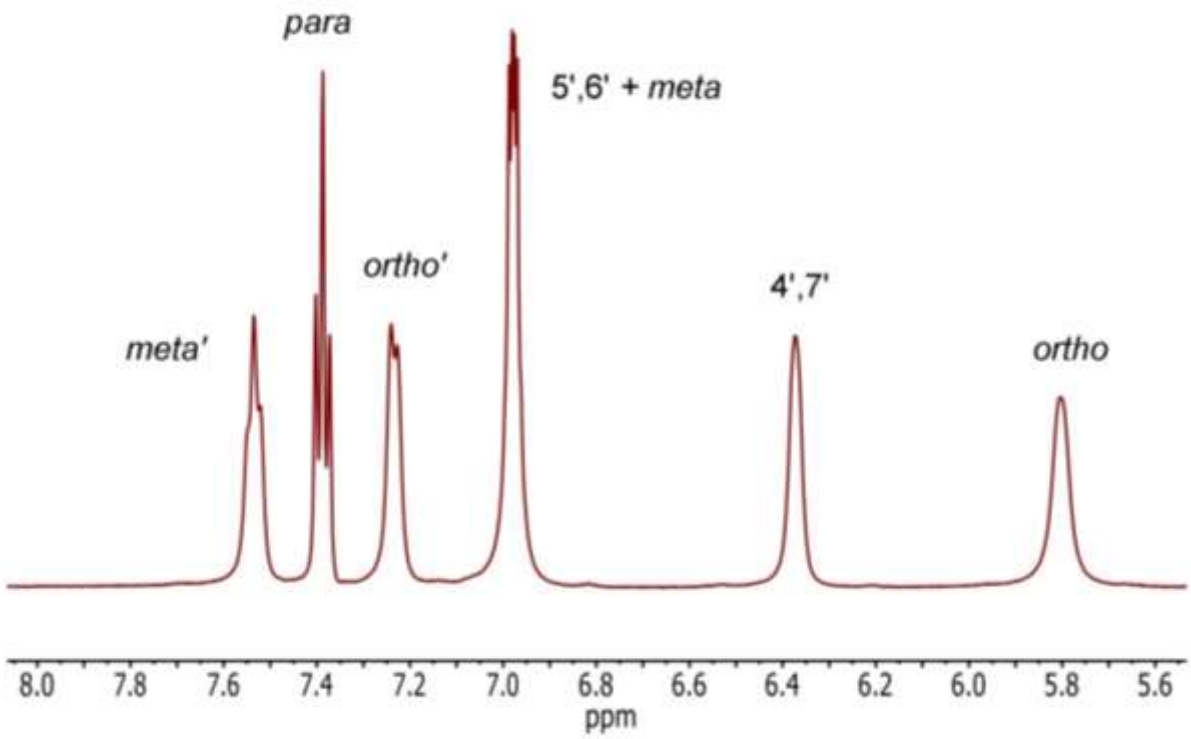

Figure 2. ^{1}H NMR spectrum for **17** at -45°C.

The *tert*-butyl benzodiazaboroles, **22** and **23**, were formed from the corresponding bromoboroles with *tert*-butyllithium in 72% and 35% yields, respectively. These compounds are much more sensitive to air and moisture than the carboranes **16**-**21**.

X-ray crystallography

Molecular structures were determined for the *ortho*-carboranes **16**, **17**, the *meta*-carboranes **18**, **19**, the *para*-carborane **21** and the *tert*-butyl benzodiazaborole **23** (Figure 3). Single crystals thereof were grown from dichloromethane or dichloromethane/*n*-hexane mixtures. Compounds **16**, **18**, **19** and **21** crystallise in the monoclinic space group *C*2/*c*, whereas **17** crystallises in the space group $P2_1/c$ and **23** in the trigonal space group $R\bar{3}$. While crystal structures of carboranes with an exopolyhedral boron atom attached to one cage carbon are known,[27] experimental geometries of carboranes with exopolyhedral boron atoms at both cage carbons have not been reported prior to this study. Dichloromethane molecules are present in the crystals structures of **16**, **17** and **21** with carborane:CH_2Cl_2 ratios of 1:1, 1:1 and 3:4 respectively. Bond lengths and angles of interest here are listed in Table 1 using the numbering schemes in Figure 1.

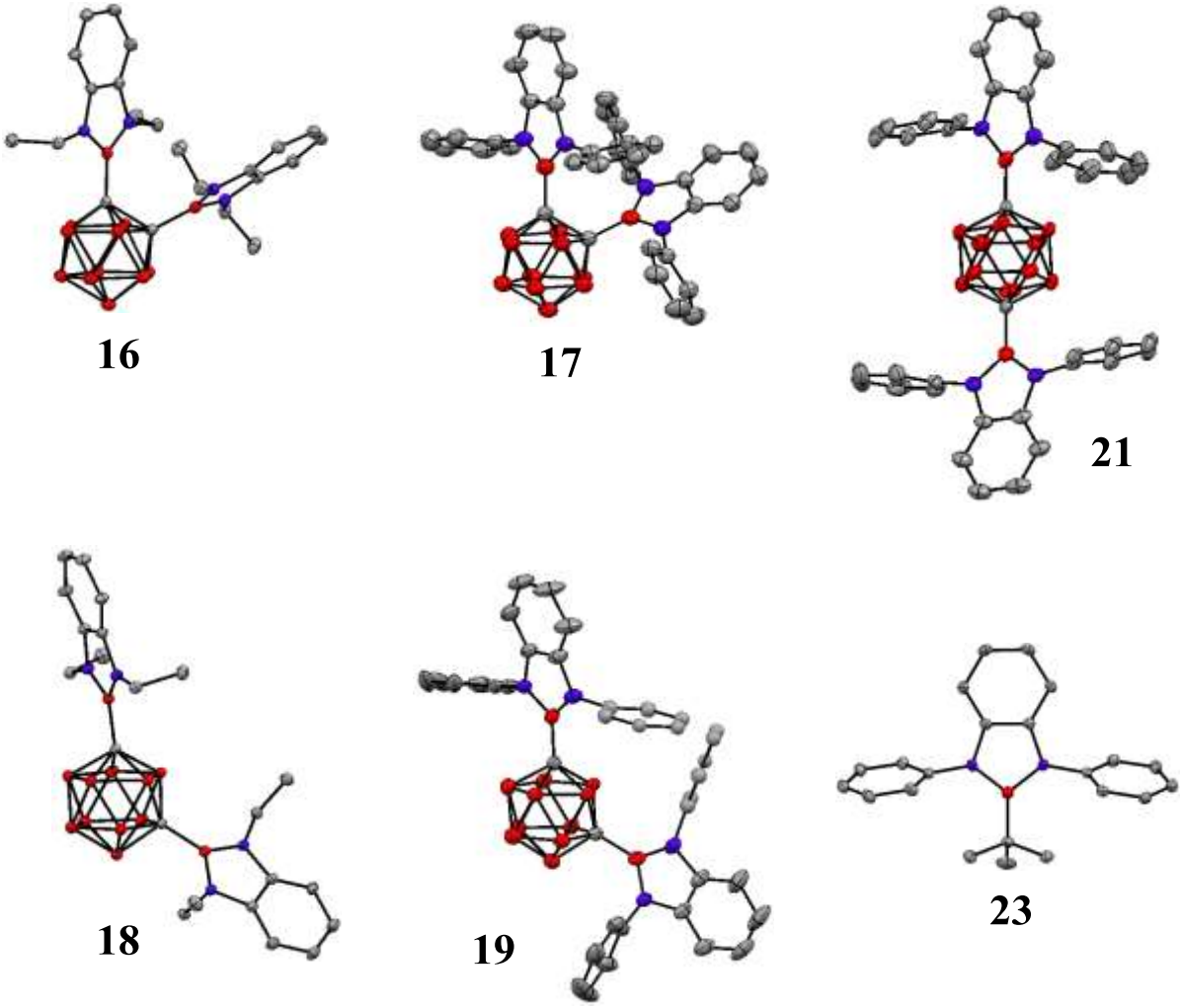

Figure 3. Molecular structures of **16** - **19**, **21** and **23**.

Table 1. Selected bond lengths (Å) for **16** - **19**, **21** and **23**.

	Bond lengths [Å]		Torsion angles [°]	Phenyl-diazaborolyl interplanar angles [°]
	C1-B2'	C1-C2	C2/B2-C1-B2'-N3'	
16	1.602(2)/ 1.602(2)	1.725(2)	76.4/57.9	-
17	1.582(4)/1.601(4)	1.697(4)	60.0/55.2	75.2/83.3/80.7/75.9
18	1.598(2)	-	95.0	-
19	1.587(3)	-	81.1	69.3
21	1.582(4)/1.585(4)/1.587(3)	-	-	86.5/80.8/75.3/82.1/84.6/84.3
23	1.587(2)	-	-	64.4/68.1

The two adjacent diazaborolyl groups in **16** and **17** adopt orientations which minimize the steric interactions between the four ethyl groups in **16** and the four phenyl groups in **17**. The observed C2-C1-B2'-N3' and C1-C2-B2"-N3" torsion angles are 76.4° and 57.9° for **16** and 60.0° and 55.2° for **17** which are smaller than in other crystal structures of *ortho*-carboranes with one diazaborolyl group at C1 and a methyl, phenyl, *tert*-butyl or a trimethylsilyl group at C2 with C2-C1-B2'-N3' torsion angles of 78-90°.[8,17]

In the crystal structure of **17** here are intramolecular C-H…π(ring) interactions between the phenyl groups with C-H…ring(centroid) distances of 2.42/2.64 Å, 3.45/3.69 Å for the C…centroid distances and 164.9/163.0° for the C-H…centroid angles (Figure 4). There are also intramolecular C-H…π(ring) interactions between the diazaborolyl rings in **17** with corresponding values of 2.78/2.82 Å, 3.31/3.36 Å and 109.9/110.5°. These interactions agree with the considerable shielding of one proton resonance at 5.81 ppm in the observed ^{1}H NMR spectrum of **17** (Figure 2). On this basis, the shielded signal is assigned to the four hydrogens attached to C2A, C2B, C2C and C2D atoms.

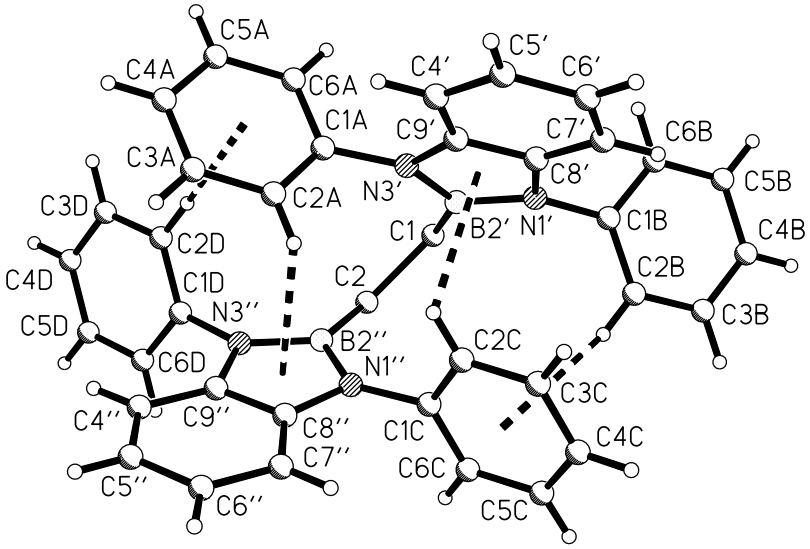

Figure 4. Intramolecular C-H…π(ring) interactions in **17**. Only C1 and C2 atoms of the carborane cluster are shown for clarity.

Each molecule of the *meta*-carboranes **18** and **19** is characterized by a two-fold axis bisecting bonds B2-B3 and B9-B10 thus placing the cage carbons C1 and C7 and the adjacent diazaborolyl fragments on symmetrically equivalent positions. Interestingly, in the *meta*-

carboranes the C1-B3 bonds (1.738(2) Å (**18**), 1.737(3) Å (**19**)) which are nearly in co-planar orientation to the diazaborolyl plane (torsion angle B3-C1-B2'-N3' = 18.8° (**18**), 5.9° (**19**)) are lengthened by ca. 0.03 Å compared to the C1-B2 bonds (1.713(2) Å (**18**), 1.704(3) Å (**19**)) which are almost perpendicular to the heterocyclic unit (torsion angle B2-C1-B2'-N3' = 95.0° (**18**), 81.1° (**19**)). Steric repulsions between the substituents at the diazaborolyl-N atoms and the B3-H unit are probably responsible for the differences in the C1-B2 and C1-B3 bonds.

The *para*-carborane **21** crystallises as a pseudo-merohedral twin with 1.33 molecules in the asymmetric unit. The half molecule is completed via a two-fold axis bisecting two opposite B-B bonds of the cage. The bonding parameters within the heterocyclic units agree with the corresponding data of numerous other 1,3,2-benzodiazaboroles.[8,16,22] In the diphenyldiazaboroles, the *N*-phenyl substituents and the diazaborolyl planes enclose interplanar angles of 64.4° in **23** to 86.5° in **21**. Thus, no conjugation between these π-systems is expected and the influence of the phenyl rings on the electronic structure of the benzodiazaborole moiety is mainly of inductive character.

As the solid-state emission data for the *meta*- and *para*-carboranes **18**-**21** differ significantly (*vide infra*), the intermolecular interactions in the crystal structures were examined here (Table 2). There are some close intermolecular phenyl C-H…π-benzodiazaborolyl interactions in the crystals of **19**, **21** and **23**. In the case of **19**, the C_6H_4 ring of the borolyl group is involved whereas in **21** and **23** the C_2N_2B rings participate in these interactions. Interactions in crystalline **18** with benzodiazaborole participation are limited to C4'H…cage B (3.09 and 3.14 Å) and C7'H…methyl H (2.26 Å).

Table 2. Intermolecular interactions in the crystal structures of **19**, **21** and **23**.

	Ring in borolyl group	Ring centroid…H distance (Å)	Ring centroid…C distance (Å)	Centroid…H-C angle (°)
19	C_6H_4	2.74	3.64	139.6
21	C_2N_2B	2.55	3.44	139.9
	C_2N_2B	2.76	3.57	131.8
	C_2N_2B	2.93	3.87	145.6
	C_2N_2B	3.04	3.93	139.8
23	C_2N_2B	2.58	3.55	148.6

Photophysics

The recorded absorption maxima in the UV-Vis spectra of solutions of **16**-**21** are devoid of any significant solvatochromism (λ = 284 - 297 nm in cyclohexane; 285 - 297 nm in dichloromethane) and agree nicely with the respective absorption data in the solid state (287 - 300 nm) (Table S2 and Figure S25). For comparison, a cyclohexane solution of 2-*tert*-butyl-1,3-diethyl-1,3,2-benzodiazaborole **22** gives rise to an intense absorption at λ = 285 nm and solid 2-*tert*-butyl-1,3-diphenyl-1,3,2-benzodiazaborole **23** absorbs at λ = 288, 293 nm (Table S2 and Figure S26). Thus the absorption bands reflect local π-π* transitions within the benzodiazaborolyl parts of the molecules.

Table 3 summarises the emission data of all compounds investigated here. The photophysical behaviour of the *ortho*-carboranes, **16** and **17**, closely resembles the characteristics of the C-mono(benzodiazaborolyl)-*ortho*-carboranes.[8,17] In cyclohexane solutions, they emit in the red to orange region at λ = 635 nm (**16**) and 579 nm (**17**) (Figure 5) with Stokes shifts of 18340 cm^{-1} (**16**) and 17330 cm^{-1} (**17**) pointing to considerable geometric reorganizations in the excited state. In dichloromethane solutions, the emission maxima are bathochromically shifted and occur at 777 nm (**16**) and 710 nm (**17**). This positive solvatochromism shows that the excited state is more polarized than the ground state. Using the Lippert-Mataga method with an Onsager-radius of 3.52 Å, transition dipole moments of 7.4 D (**16**) and 7.7 D (**17**) were estimated which agrees with the distinct charge transfer (CT) character of these low-energy emissions. In addition, weaker emission bands were measured for cyclohexane solutions of compounds **16** and **17** in the UV region (λ = 330 nm (**16**), 346 nm (**17**)). As evidenced by X-ray crystallography, the molecules adopt conformations with C2-C1-B2'-N3' torsion angles markedly different from 90°. This rotational mobility around the C1-B2 bond opens a path to an alternative excited state characterized by minor geometric changes.[8] Fluorescence quantum yields for both emissions are very low in solution (Φ_F <1 %).

In the solid state, the low-energy emissions of the *ortho*-carboranes **16** and **17,** were bathochromically shifted with respect to the corresponding maxima in cyclohexane at λ = 666 nm (**16**) and 618 nm (**17**) (Figures 5 and 6). Due to restriction of molecular motions, the solid state quantum yields (Φ_F 3 % (**16**), 14 % (**17**)) are higher than in solution. However, they are significantly lower than the reported Φ_F values between 25 and 70 % for luminescent mono(benzodiazaborolyl)-*ortho*-carboranes with large C2-C1-B2'-N3' torsion angles of 78-

90°.[8,17] Non-radiative decay processes are obviously favorable in the bis(benzodiazaborolyl)-*ortho*-carboranes, **16** and **17**, which may be due to the smaller C2-C1-B2'-N3' torsion angles (56-76°) in their crystal structures.

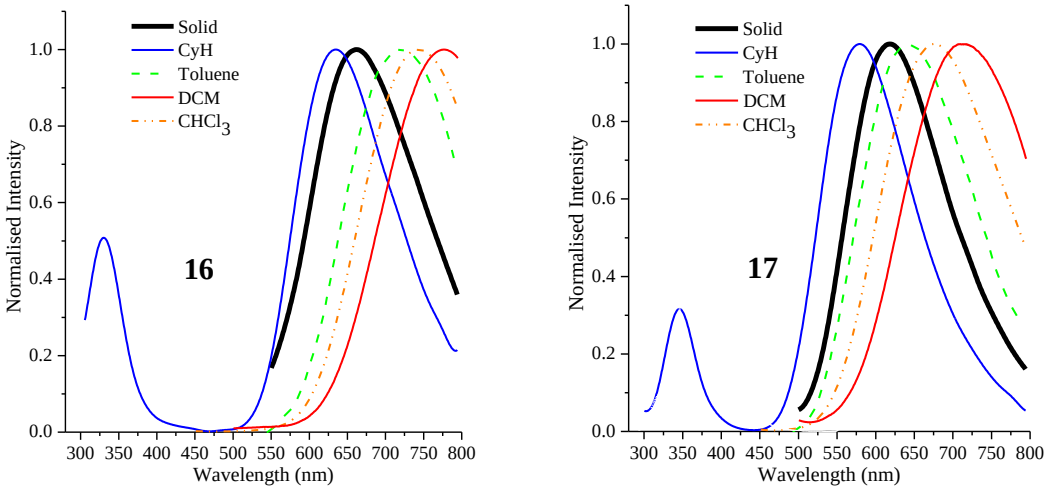

Figure 5. Emission spectra of *ortho*-carboranes **16** and **17**.

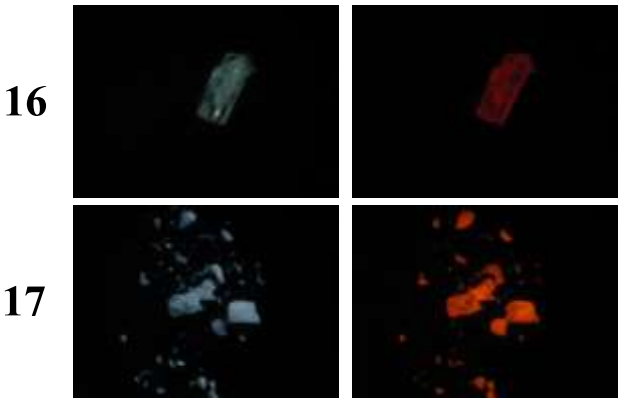

Figure 6. Crystals of **16** and **17**. Left column: Without UV irradiation. Right column: Under UV irradiation at 350 nm.

Table 3. Emission data for **16 – 23**.

	Cyclohexane				Dichloromethane (DCM)				Solid state			
	Emission λ_{max} [nm]	Relative Height	Stokes shift [cm^{-1}]	Φ_F [%]	Emission λ_{max} [nm]	Relative Height	Stokes-shift [cm^{-1}]	Φ_F [%]	Emission λ_{max} [nm]	Stokes shift [cm^{-1}]	Φ_F[a] [%]	Lifetime τ_F [ns]
16	330, 635	0.51 : 1.00	3790, 18340	1	777		21290	< 1	666	18720	3	2.5 ± 0.2
17	346, 579	0.32 : 1.00	5520, 17330	1	710		20670	< 1	618	18200	14	2.3 ± 0.1
18	309, 392	1.00 : 0.02	1700, 9830	26	309, 487	1.00 : 0.56	2170, 15170	2	474	13320	< 1	2 ± 1[b]
19	303		1440	1	306, 455	1.00 : 0.03	1790, 13210	1	310	1770	28	1.8 ± 0.2
20	310		1430	41	314, 461	1.00 : 0.15	1860, 12720	< 1	314, 377[c]	1560, 8320	9	[d]
21	303		1450	3	307		1750	1	354	5980	72	3.4 ± 0.2
22	307[e]		1440	[f]	309[e,g]		1650	[f]	[h]			
23	[h]				[h]				312	2080	12	[f]

[a] Measured with the integrating sphere method.

[b] Large error due to low intensity.

[c] Relative height 1.00 : 0.09.

[d] Biexponential fit necessary with values of 1.0 ± 0.2 and 4.6 ± 0.2 determined.

[e] Reference 23.

[f] Not recorded.

[g] Not recorded in DCM, values are quoted with tetrahydrofuran (THF) which has a similar solvent polarity.

[h] Reliable measurements were not obtained due to photochemical decomposition of sample.

For the cyclohexane solutions of *meta*- and *para*-carboranes **18**-**21**, high energy (UV) emission bands were observed (λ = 303 - 310 nm) (Figures 7 and 8) without a significant solvatochromism upon changing the solvent to dichloromethane (λ = 306 - 314 nm). Together with the reference compound 2-*tert*-butyl-1,3-diethyl-1,3,2-benzodiazaborole **22** which emits at 307 nm in cyclohexane and 309 nm in THF (Figure S26), this allows the conclusion that the UV emissions arise from local π-π* transitions within the benzodiazaborolyl units. The small Stokes shifts of 1430 - 1700 cm^{-1} for the high-energy emissions from **18**-**22** indicate negligible geometric rearrangement in the excited state. The Φ_F values of the two diethylbenzodiazaborolyl compounds **18** (26 %) and **20** (41 %) in cyclohexane solutions are significantly higher than those of their diphenyl analogues **19** (1 %) and **21** (3 %). In other solvents, the quantum yields are lower for all four compounds and decrease to values of 2 % and below in dichloromethane (Table S5).

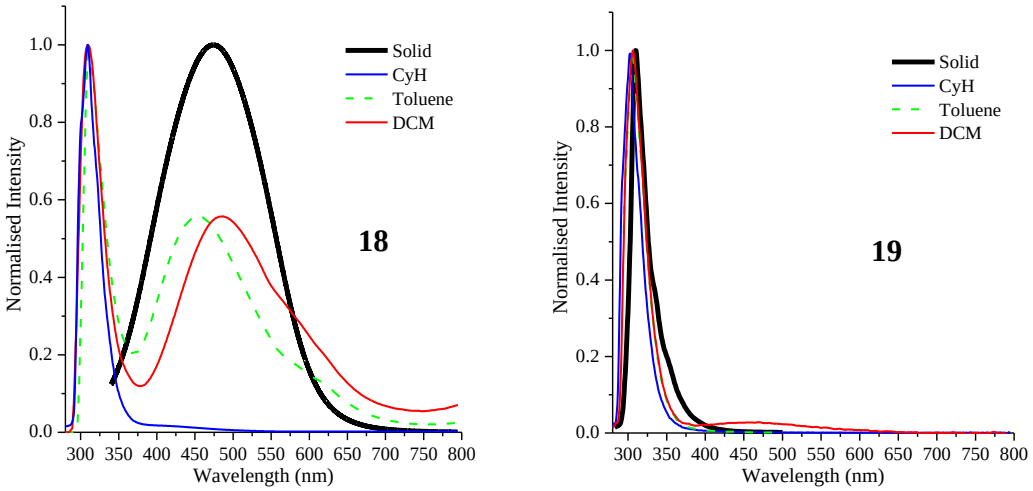

Figure 7. Emission spectra of *meta*-carboranes **18** and **19**.

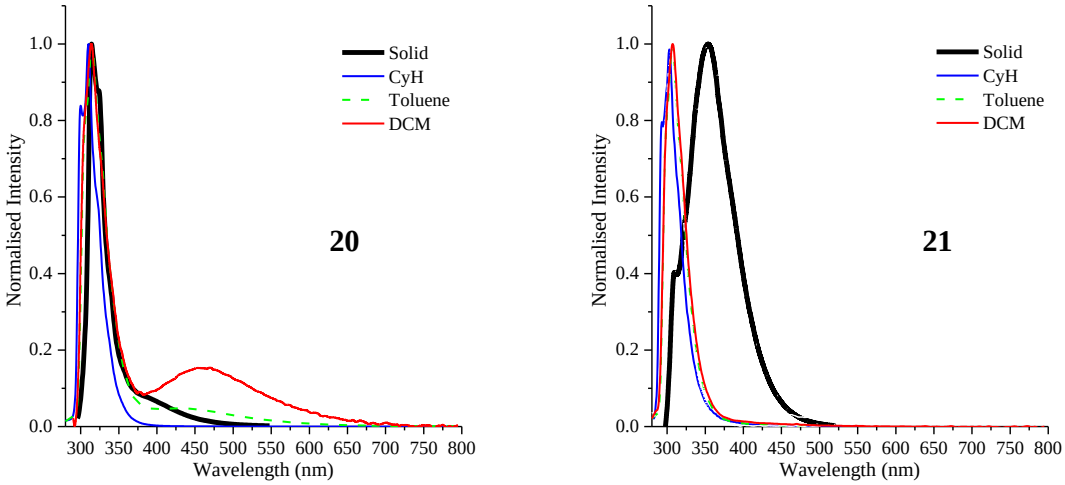

Figure 8. Emission spectra of *para*-carboranes **20** and **21**.

Interestingly, additional emission bands at lower energies were detected for **18** in cyclohexane, toluene and dichloromethane, for **19** in dichloromethane and for **20** in toluene and dichloromethane (Figures 7 and 8 and Tables S3-6). These bands have markedly lower intensities compared to the high-energy emissions and reach into the blue region of the visible spectrum (λ = 455 - 487 nm in dichloromethane). Solvatochromic shifts of 2580 cm^{-1} for **18** and 1330 cm^{-1} for **20** upon changing the solvent from toluene to dichloromethane agree with a CT character of these emissions. The Stokes shifts of 12720 - 15170 cm^{-1} in dichloromethane point to considerable structural changes in the excited state which, however, are less pronounced than for the *ortho*-carboranes **16** and **17**. The fact that CT emission for the diphenylbenzodiazaborolyl compounds was only found in the case of **19** in the polar solvent dichloromethane may be explained by the lower donor strengths of the diphenylbenzodiazaborolyl group compared to the diethylbenzodiazaborolyl group.

Unusual luminescence data were obtained from solid *meta*- and *para*-carboranes **18** - **21**. Only one emission band was measured in case of both *meta*-carboranes. For **18**, this band was found in the blue region (λ = 474 nm) and therefore presumably corresponds to the CT emission which was also observed in solution (Figure 7). The solid state emission for **19** at λ = 310 nm is assigned to a local emission within the benzodiazaborolyl unit. The solid *para*-carborane derivative **20** shows a band for a local transition at λ = 314 nm and another band of lower intensity at λ = 377 nm. For **21**, an emission band occurred at λ = 354 nm which is considerably bathochromically shifted compared to the emission in cyclohexane at λ = 303 nm. The large energy difference of 4750 cm^{-1} in the emission maxima between the solution and the solid state for **21** suggests the existence of two different excited states for **21**.

The solid state quantum yields of the diphenylbenzodiazaborolyl compounds **19** (Φ_F 28 %) and **21** (Φ_F 72 %) are significantly higher than those of their diethyl analogues **18** (Φ_F < 1 %) and **20** (Φ_F 9 %). Aggregation of the diethylbenzodiazaborolyl compounds **18** and **20** may have led to quenching of luminescence whereas restriction of molecular motions in solid diphenylbenzodiazaborolyl compounds **19** and **21** reduced non-radiative decay.

Luminescence lifetimes of 1.0 - 4.6 ns of the solids of **16** - **21**, clearly show that the observed emissions arise from fluorescence (Table 3). The emissions generally decayed monoexponentially with the exception of **20**. In this case a biexponential fit was necessary which means that two fluorescence processes occurred for solid **20**. This agrees with the two observed emission bands. Thus two different excited states are populated in case of this compound.

Although no direct information about packing of the molecules in the spectroscopically investigated solid layers is available, it is conceivable that similar intermolecular interactions as described in the crystallographic section contribute to the differences in the solid state photophysical behaviour of **18-21**.

Electrochemistry

Cyclic voltammetry for the carboranes **16-21** in dichloromethane solutions reveals irreversible oxidation waves in the narrow range between 0.9-1.0 V with respect to the ferrocene/ferrocenium couple (Figure S27) which are characteristic of oxidations of the benzodiazaborolyl group.[20] Reduction waves were observed for the *ortho*-carboranes, **16** and **17**, but not for the *meta*- and *para*-carboranes, **18-21**. The *ortho*-carboranes are considerably easier to reduce than their *meta*- and *para*-carborane analogues. The two one-electron reduction waves observed for **16** in acetonitrile (shown in Figure 9) are typical for 1,2-diaryl-*ortho*-carboranes.[16,28,29] CV simulations of these two reversible 1e reduction processes (Figure 9) gave values of the heterogeneous electron transfer like those of diphenyl-*ortho*-carborane, 1,2-Ph_2-1,2-$C_2B_{10}H_{10}$ **24**, observed in acetonitrile.[16,28] Compound **17** is, unfortunately, not soluble in acetonitrile.

In dichloromethane solutions, two quasi-reversible reduction processes are observed for **16** and **17**, and the mechanism is reasonably well described by digital simulations (Figures S28 and S29) in which the first reduction process is slower than the second, in a similar way as observed for **24** in the same solvent (Figure S30). It is generally accepted that a slow electron transfer indicate a geometrical rearrangement and/or molecular reorganization induced by the electron transfer process.[30]

The CV data for electrochemical reduction waves for **16**, **17** and **24** summarized in Table 4 are similar and suggest that both, the phenyl- and benzodiazaborolyl groups, have comparable influences on the stabilities of the unusual 2n+3 carborane radical monoanions. From a recent electrochemical study on monobenzodiazaborolyl carboranes, the long C1-C2 cluster bond lengths facilitate the stabilities of the monoanionic radicals.[17] The structurally determined C1-C2 bond lengths for **16**, **17** and **24** are in fact similar [1.725(2), 1.707(3) and 1.722-1.730(2) Å respectively].[28]

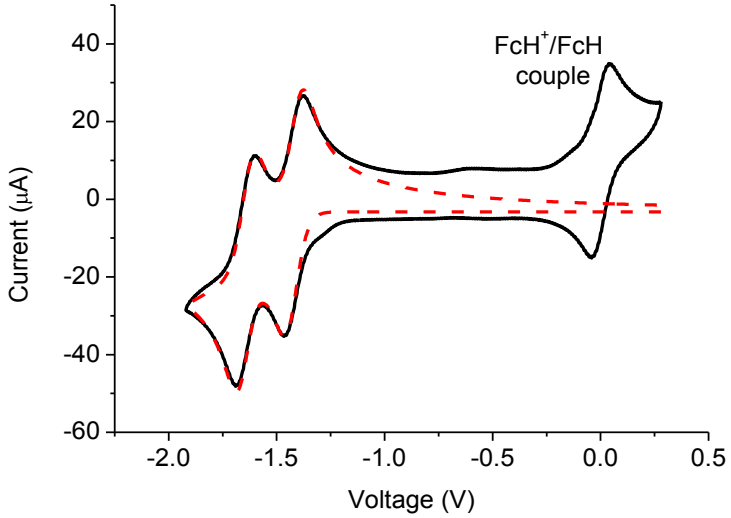

Figure 9. Experimental (black solid line) and simulated (red dashed line, Redox(0/-1): E°=-1.418 V, k°=2.5×10^{-3} cm/s, α=0.50; Redox(-1/-2): E°=-1.644 V, k°=2.5×10^{-3} cm/s, α=0.50) CV of **16** in acetonitrile. Potentials are against the FcH^+/FcH redox couple (not simulated).

Table 4. Reduction potentials from cyclic voltammetry data[a] of **16**, **17** and **24**.

	Working Electrode [b]	Solvent	E(Red1) cathodic V [c]	E(Red1) anodic V[d]	$E_{1/2}$ (Red1) V	Red1 p-p mV[e]	E(Red2) cathodic V[f]	E(Red2) anodic V [g]	$E_{1/2}$ (Red2) V	Red2 p-p mV[e]	$E_{1/2}$(Red1-Red2) mV
16	GC	MeCN	-1.46	-1.37	-1.42	90	-1.69	-1.60	-1.65	90	230
	Pt	DCM	-1.88	-1.49	-1.69	390	-1.88	-1.77	-1.83	110	140
17	Pt	DCM	-2.41	-1.51	-1.96	900	-2.41	-1.75	-2.08	660	120
24	GC	MeCN	-1.63	-1.50	-1.57	130	-1.76	-1.68	-1.72	80	155
	Pt	DCM	-1.90	-1.48	-1.69	420	-1.90	-1.80	-1.85	100	160

[a] 0.1 M $^{n}Bu_4NPF_6$ solution at 298 K, scan rate 100 mV s^{-1}, referenced internally to the ferrocene/ferrocenium FcH/FcH^+ couple, with platinum wires as counter and reference electrodes. Measurements carried out under inert atmosphere using a glove box.
[b] GC = glassy carbon working electrode, Pt = platinum working electrode
[c] cathodic wave of first one-electron reduction wave.
[d] anodic wave of first one-electron reduction wave.
[e] peak separation.
[f] cathodic wave of second one-electron reduction wave.
[g] anodic wave of second one-electron reduction wave.

Computations

The molecular geometries of all eight compounds, **16 - 23**, were optimized at B3LYP/6-31G* with no symmetry constraints. Calculated GIAO ^{11}B NMR shifts from these geometries are in very good agreement with experimental NMR data for **16**-**21** (Table S7). The computed GIAO ^{1}H NMR shifts of 7.36 and 6.39 ppm for the two sets of *ortho*-protons on the optimised geometry of **17** correspond well with the observed data (Figure 2). The geometric parameters for **16**-**19**, **21** and **23** are in general agreement with the results of the X-ray determinations. Rotation barrier energies at the C1-B2' axis for **16** and were estimated to be 7.4 and 13.0 kcal·mol^{-1}, respectively. These values are probably underestimated, especially for **17**, as the computed C1-C2 bond lengths in the optimized geometries are 1.753 and 1.746 Å compared to the experimental values of 1.725(2) and 1.707(3) Å for **16** and **17**, respectively.

The different C1-B2 and C1-B3 bond lengths found in the X-ray structure analyses as well as in the optimised geometries of the *meta*-carboranes, **18** and **19**, are due to steric effects of the ethyl and phenyl groups at N1' and N3'. Replacing the ethyl substituents in **18** with hydrogen atoms gave an optimised geometry with identical C1-B2 and C1-B3 bond lengths.

The frontier orbital energies for **16**-**24** are given in Table 5. The orbital energies for the simple molecules, *ortho*-, *meta*- and *para*-carboranes, and the parent diazaboroles are also included for comparison. The HOMOs in the boroles are represented by the π orbitals of the benzodiazaborolyl unit as shown in Figure 10 for **16** and **18**. For **16**-**21**, the LUMOs are the π*B orbitals with some carborane character. The LUMOs for the diazaboroles **22** and **23** are of π*(benzodiazaborolyl) character. The similarities in the frontier orbital energies between the carboranes **18**-**21** and the simpler benzodiazaboroles including **22** and **23** agree nicely with the experimental UV spectra where similar low energy transitions within the benzodiazaborole were observed.

Table 5. Frontier orbital energies for **16-24** and related compounds.

		LUMO [eV]	HOMO [eV]	HOMO-LUMO Gap [eV]
1,2-$[C_6H_4(NEt)_2B]_2$-*ortho*-$C_2B_{10}H_{10}$	**16**	-0.93	-5.78	4.85
1,2-$[C_6H_4(NPh)_2B]_2$-*ortho*-$C_2B_{10}H_{10}$	**17**	-0.77	-5.85	5.08
1,7-$[C_6H_4(NEt)_2B]_2$-*meta*-$C_2B_{10}H_{10}$	**18**	-0.47	-5.61	5.14
1,7-$[C_6H_4(NPh)_2B]_2$-*meta*-$C_2B_{10}H_{10}$	**19**	-0.43	-5.60	5.17
1,12-$[C_6H_4(NEt)_2B]_2$-*para*-$C_2B_{10}H_{10}$	**20**	-0.52	-5.54	5.02
1,12-$[C_6H_4(NPh)_2B]_2$-*para*-$C_2B_{10}H_{10}$	**21**	-0.31	-5.58	5.27
$C_6H_4(NEt)_2B$*t*Bu	**22**	-0.28	-5.25	4.97
$C_6H_4(NPh)_2B$*t*Bu	**23**	-0.25	-5.38	5.13
1,2-Ph_2-*ortho*-$C_2B_{10}H_{10}$	**24**	-1.40	-7.18	5.78
ortho-$C_2B_{10}H_{12}$		-0.25	-8.59	8.34
meta-$C_2B_{10}H_{12}$		-0.09	-8.61	8.52
para-$C_2B_{10}H_{12}$		-0.05	-8.64	8.59
$C_6H_4(NEt)_2BH$		-0.23	-5.37	5.14
$C_6H_4(NPh)_2BH$		-0.22	-5.54	5.32

The *ortho*-carboranes **16** and **17** have lower HOMO and LUMO energies by 0.2-0.7 eV compared to **18**-**23**. Reduction waves were observed for **16** and **17,** but not for **18**-**21,** in the cyclic voltammetry studies here which corresponds to the lower LUMO energies computed for the *ortho*-carboranes. However, the calculated LUMO energy for the diphenyl carborane **24** is lower than for **16** by 0.4 eV yet they have similar reduction potentials observed experimentally (Table 4). Thus, care should be exercised when comparing observed reduction potentials with computed LUMO energies.[17]

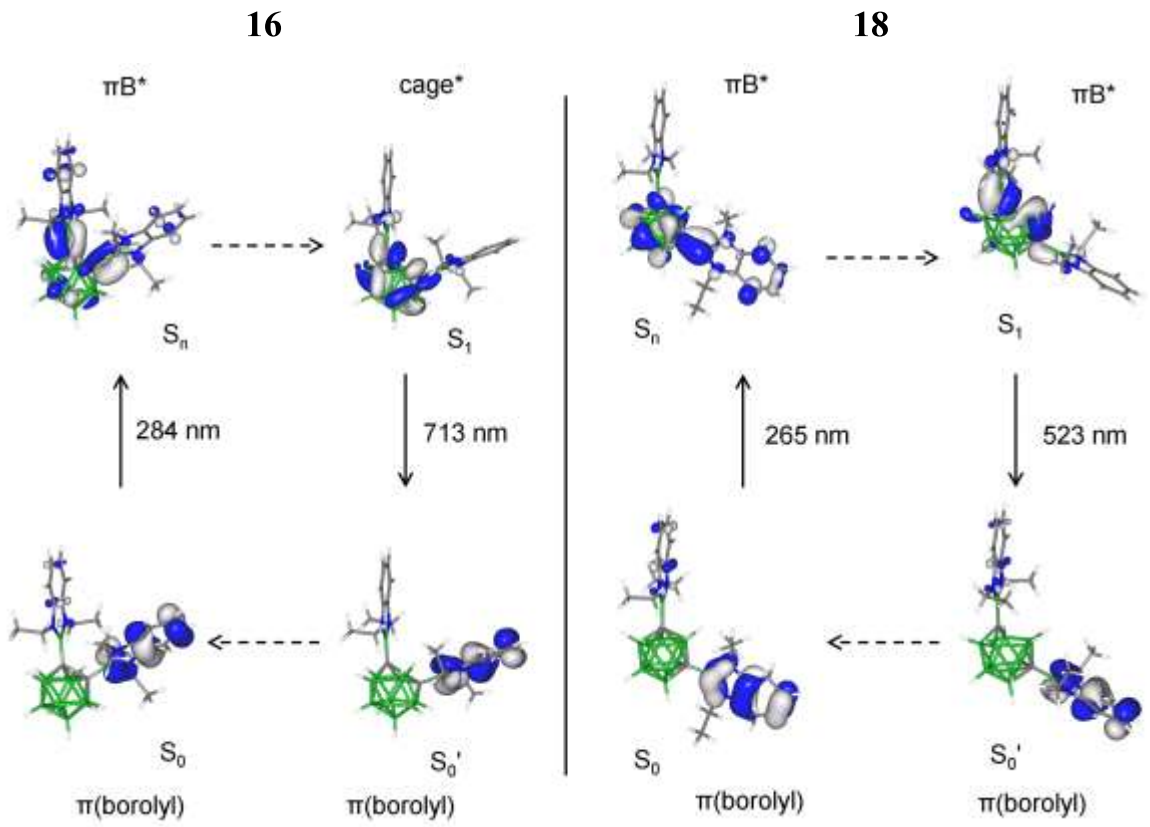

Figure 10. Molecular orbitals involved in the absorption and low-energy emission processes for **16** and **18**.

TD-DFT calculations on these geometries predict π(borolyl) > πB* transitions with high oscillator strengths (*f* = 0.094 to 0.485) for all carboranes **16-21** (Table S8, Figure 10). There are also borolyl group to phenyl group transitions in **17**, **19** and **21** but with low oscillator strengths. The computed transition energies are in broad agreement with the absorption data for all carboranes and the observed bands at ca. 292 nm are confidently assigned here as π(borolyl) > πB* transitions. The absorption bands for the *tert*-butyl compounds **22** and **23** are attributed to π(benzodiazaborolyl) > π*(benzodiazaborolyl) transitions.

The low-energy emissions for the *ortho*-carboranes **16** and **17** arise from the charge transfer of the cage to the diazaborolyl unit. The computed first excited state geometry (S_1) for **16** has a long C1-C2 bond distance of 2.45 Å. Thereby, the LUMO is located on the cage and the HOMO on the borolyl group. The data of the weak low-energy emission observed for the *meta*- and *para*-carboranes **18-20** also suggest some charge transfer character thus implying cluster rearrangements in the excited states of the molecules. The computed first excited state geometry (S_1) for **18** in Figure 10 displays a somewhat disordered *meta*-carborane cluster with

long C1-B2/B3 bond distances of 2.25 Å. The computed LUMO on this S_1 geometry showed a πB* type orbital with considerable cage character. The calculated $S_0 < S_1$ emission values of 723 nm and 523 nm for **16** and **18** respectively, are in reasonable agreement with observed solid state values of 666 nm and 474 nm.

Conclusions

A general route from bromobenzodiazaboroles and dilithiated carboranes to novel *ortho*-, *meta*- and *para*-carboranes (**16**-**21**) containing 1,3,2-benzodiazaborolyl groups at both cage carbons is presented. According to the photophysical data, two different excited states are possible for all three carborane isomers, the population of which depends on the solvent or the solid state, respectively. These excited states either correspond to local excitations within the benzodiazaborolyl fragment or to charge transfer (CT) processes between the heterocyclic unit and the cage. Huge Stokes shifts of 17330 and 21290 cm^{-1} for the CT emissions of **16** and **17** underline the unique characteristics of the *ortho*-carborane cage. This is most certainly due to its flexible C-C bond and its increased electron-deficiency compared to the other carborane isomers. In agreement with these factors, electrochemical reduction waves were observed for the *ortho*-carboranes, **16** and **17**, but not for the *meta* and *para* carboranes, **18**-**21**. However, the weak low-energy emissions observed for **18**-**21** indicate that the *meta*- and *para*-carborane clusters are also active participants in light-induced charge transfer with the heterocyclic substituents. To the best of our knowledge, such low-energy CT emissions have not been reported for *meta*- and *para*-carboranes previously.

Experimental Section

General: All manipulations were performed under an atmosphere of dry oxygen-free argon using Schlenk techniques. All solvents were dried by standard methods and freshly distilled prior to use. The compounds 2-bromo-1,3-diethyl-1,3,2-benzodiazaborole[31] and 2-bromo-1,3-diphenyl-1,3,2-benzodiazaborole[23] were prepared as described in the literature. 1,2-, 1,7- and 1,12-dicarbadodecaborane (*ortho*-, *meta*- and *para*-carborane respectively) were purchased commercially (KatChem). NMR spectra were recorded from solutions at room temperature on a Bruker AM Avance DRX500 (^1H, ^{11}B, ^{13}C), a Bruker Avance III 500 and a Bruker Avance 400 Spectrometer ($^1H\{^{11}B\}$) with $SiMe_4$ (^1H, ^{13}C) and $BF_3{\cdot}OEt_2$ (^{11}B) as external standards. ^1H- and $^{13}C\{^1H\}$ NMR spectra were calibrated on the solvent signal [$CDCl_3$: 7.24 (^1H), 77.16 (^{13}C); C_6D_6: 7.15 (^1H), 128.06 (^{13}C)]. ^1H, $^1H\{^{11}B\}$, $^{13}C\{^1H\}$ and $^{11}B\{^1H\}$ NMR spectra for

carboranes **16** - **21** are shown in Figures S1-S24. The ^{1}H and ^{13}C NMR peaks were assigned with the aid of 2D ^{1}H-^{1}H COSY and ^{1}H-$^{13}C\{^{1}H\}$ correlation spectra. Mass spectra were recorded with a VG Autospec sector field mass spectrometer (Micromass).

1,2-Bis-(1´,3´-diethyl-1´,3´,2´-benzodiazaborol-2´-yl)-1,2-dicarbadodecaborane (16): A solution of 2-bromo-1,3-diethyl-1,3,2-benzodiazaborole (0.92 g, 3.64 mmol) in *n*-hexane (13 mL) was added dropwise to a chilled slurry (0 °C) of 1,2-dilithio-1,2-dicarbadodecaborane, prepared from 1,2-dicarbadodecaborane (0.26 g, 1.80 mmol) and an *n*-butyllithium solution (1.6 M in *n*-hexane, 2.40 mL, 3.84 mmol) in diethyl ether (8.5 mL). The mixture was stirred for 19 h at ambient temperature and filtered subsequently. The filter cake was washed with *n*-hexane (2 × 3 mL), freed from volatile materials *in vacuo*, taken up in dichloromethane (10 mL) and filtered again. The filtrate was evaporated to dryness. Final purification of the residue was achieved by short-path distillation at $5 \cdot 10^{-3}$ mbar by means of a flame followed by crystallisation from a 1:1 mixture (24 mL) of dichloromethane and *n*-hexane to afford a colorless solid **16**. Yield: 0.43 g (42 %). Found: C, 48.16; H, 6.97; N 9.80 %; $C_{22}H_{38}B_{12}N_4 \cdot CH_2Cl_2$ requires C, 48.19; H, 7.03; N, 9.77 %; ^{1}H NMR (C_6D_6): δ [ppm] = 0.92 (t, ^{3}J = 6.9 Hz, 12 H, CH_3), 2.0 - 4.0 (m, br, 10 H, BH), 3.57 (q, ^{3}J = 6.9 Hz, 8 H, CH_2), 6.64 (m, 4 H, H4´,7´), 6.92 (m, 4 H, H5´,6´); ^{1}H NMR ($CDCl_3$): δ [ppm] = 1.23 (t, ^{3}J = 7.1 Hz, 12 H, CH_3), 2.0 - 4.0 (m, br, 10 H, BH), 3.57 (q, ^{3}J = 7.1 Hz, 8 H, CH_2), 6.99 (m, 8 H, H4´,5´,6´,7´); $^{1}H\{^{11}B\}$ NMR ($CDCl_3$): δ [ppm] = 2.49 (s, 4 H, BH), 2.64 (s, 4 H, BH), 3.34 (s, 2 H, BH); $^{13}C\{^{1}H\}$ NMR (C_6D_6): δ [ppm] = 15.3 (s, CH_3), 37.8 (s, CH_2), 71.0 (br s, C1), 110.3 (s, C4´,7´), 120.7 (s, C5´,6´), 136.2 (s, C8´,9´); $^{13}C\{^{1}H\}$ NMR ($CDCl_3$): δ [ppm] = 15.5 (s, CH_3), 37.9 (s, CH_2), 70.5 (br s, C1), 110.1 (s, C4´,7´), 120.3 (s, C5´,6´), 136.0 (s, C8´,9´); $^{11}B\{^{1}H\}$ NMR (C_6D_6): δ [ppm] = –8.4 (with shoulder at -8.9 ppm, 6B), –5.2 (2B), 2.5 (2B), 22.9 (2B, B2',2"); $^{11}B\{^{1}H\}$ NMR ($CDCl_3$): δ [ppm] = –9.1 (6B), –5.8 (2B), 1.8 (2B), 22.9 (2B, B2',2"); MS (EI): m/z = 488.3 (M^+), 472.3 (M^+-CH_3), 459.3 (M^+-C_2H_5), 244.2 (M^{2+}).

1,2-Bis-(1´,3´-diphenyl-1´,3´,2´-benzodiazaborol-2´-yl)-1,2-dicarbadodecaborane (17): A solution of 2-bromo-1,3-diphenyl-1,3,2-benzodiazaborole (1.50 g, 4.30 mmol) in benzene (11 mL) was added dropwise to a chilled slurry (0 °C) of 1,2-dilithio-1,2-dicarbadodecaborane, prepared from 1,2-dicarbadodecaborane (0.31 g, 2.15 mmol) and an *n*-butyllithium solution (1.6 M in *n*-hexane, 2.82 mL, 4.51 mmol) in diethyl ether (10 mL). The mixture was stirred for 65 h at ambient temperature and filtered subsequently. The filter cake was washed with *n*-

hexane (2 × 3 mL), and the combined filtrates were freed from volatiles *in vacuo*. Purification of the residue was achieved by short-path distillation at $5 \cdot 10^{-3}$ mbar by means of a flame followed by crystallisation from dichloromethane (25 mL). For complete removal of the dichloromethane included in the crystals, they were heated *in vacuo* with a heat gun until gas evolution ceased. Yield: 0.46 g of colourless solid **17** (31 %). Found: C, 67.18; H, 5.57; N, 8.23 %; $C_{38}H_{38}B_{12}N_4$ requires C, 67.07; H, 5.63; N, 8.23 %; ^{1}H NMR ($CDCl_3$, 293 K): δ [ppm] = 1.0 - 3.5 (m, br, 10 H, BH), 5.90 (s, br, 4 H, H_{ortho}), 6.34 (m, 4 H, H4´,7´), 6.95 (m, 4 H, H5´,6´), 6.98 (s, br, 4 H, H_{meta}), 7.20 (s, br, 4 H, $H_{ortho'}$), 7.36 (t, ^3J = 7.2 Hz, 4 H, H_{para}), 7.50 (s, br, 4 H, $H_{meta'}$); ^{1}H NMR ($CDCl_3$, 228 K): δ [ppm] = 1.0 - 3.5 (m, br, 10 H, BH), 5.81 (s, br, 4 H, H_{ortho}), 6.37 (br, 4 H, H4´,7´), 6.98 (m, 4 H, H5´,6´ + s, br, 4 H, H_{meta}), 7.23 (d, ^3J ~ 6.6 Hz, 4 H, $H_{ortho'}$), 7.38 (t, ^3J = 7.5 Hz, 4 H, H_{para}), 7.53 (t, ^3J ~ 6.7 Hz, 4 H, $H_{meta'}$); ^{1}H{^{11}B}-NMR ($CDCl_3$): δ [ppm] = 1.64 (s, 4 H, B4,5,7,11H), 2.01 (s, 2 H, BH), 2.11 (s, 2 H, BH), 2.55 (s, 2 H, BH); ^{13}C{^{1}H} NMR ($CDCl_3$): δ [ppm] = 69.5 (br s, C1), 111.4 (s, C4´,7´), 121.1 (s, C5´,6´), 127.8 (s, C_{para}), 128.8 (s, br, C_{ortho}), 129.1 (s, br, C_{meta}), 129.5 (s, br, $C_{meta'}$), 130.1 (s, br, $C_{ortho'}$), 138.0 (s, C8´,9´), 140.0 (s, C_{ipso}); ^{11}B{^{1}H} NMR ($CDCl_3$): δ [ppm] = –9.7 (6 B), –6.2 (2 B), 1.0 (2 B), 23.2 (2 B, B2',2"); MS (EI): m/z = 680.8 (M^+), 411.0 (M^+-$B(NPh)_2C_6H_4$), 339.9 (M^{2+}).

1,7-Bis-(1´,3´-diethyl-1´,3´,2´-benzodiazaborol-2´-yl)-1,7-dicarbadodecaborane (18): A solution of 2-bromo-1,3-diethyl-1,3,2-benzodiazaborole (0.74 g, 2.93 mmol) in *n*-hexane (10 mL) was added dropwise to a chilled slurry (0 °C) of 1,7-dilithio-1,7-dicarbadodecaborane, prepared from 1,7-dicarbadodecaborane (0.21 g, 1.46 mmol) and an *n*-butyllithium solution (1.6 M in *n*-hexane, 1.90 mL, 3.04 mmol) in diethyl ether (8.0 mL). The mixture was stirred for 20 h at ambient temperature and filtered subsequently. The filter cake was washed with *n*-hexane (12 mL).The combined filtrates were freed from volatiles *in vacuo*. Purification of the residue was achieved by short-path distillation at $5 \cdot 10^{-3}$ mbar by means of a flame followed by crystallisation from a mixture of dichloromethane (12 mL) and *n*-hexane (10 mL) to yield colourless solid **18**. Yield: 0.25 g (35 %). Found: C, 53.94; H, 7.87; N, 11.39 %; $C_{22}H_{38}B_{12}N_4$ requires C, 54.11; H, 7.84; N, 11.47 %; ^{1}H NMR ($CDCl_3$): δ [ppm] = 1.34 (t, ^3J = 6.9 Hz, 12 H, CH_3), 1.8 - 3.7 (m, br, 10 H, BH), 4.00 (q, ^3J = 6.9 Hz, 8 H, CH_2), 7.07 (m, 8 H, H4´,5´,6´,7´); ^{1}H{^{11}B} NMR ($CDCl_3$): δ [ppm] = 2.43 (s, 2 H, BH), 2.68 (s, 4 H, B4,6,8,11H), 2.75 (s, 2 H, BH), 3.16 (s, 2 H, BH); ^{13}C{^{1}H} NMR ($CDCl_3$): δ [ppm] = 16.0 (s, CH_3), 37.9 (s, CH_2), 63.5 (br s, C1), 109.6 (s, C4´,7´), 119.9 (s, C5´,6´), 136.5 (s, C8´,9´); ^{11}B{^{1}H} NMR

($CDCl_3$): δ [ppm] = –12.5 (2B), –9.3 (4 B, B4,6,8,11), –8.0 (2 B), –1.2 (2 B), 24.0 (2B, B2',2''); MS (EI): m/z = 488.4 (M^+), 471.3 (M^+-CH_3), 244.2 (M^{2+}).

1,7-Bis-(1´,3´-diphenyl-1´,3´,2´-benzodiazaborol-2´-yl)-1,7-dicarbadodecaborane (19): A solution of 2-bromo-1,3-diphenyl-1,3,2-benzodiazaborole (1.59 g, 4.57 mmol) in benzene (10 mL) was added dropwise to a chilled slurry (0 °C) of 1,7-dilithio-1,7-dicarbadodecaborane, prepared from 1,7-dicarbadodecaborane (0.33 g, 2.29 mmol) and an *n*-butyllithium solution (1.6 M in *n*-hexane, 3.00 mL, 4.80 mmol) in diethyl ether (10 mL). The mixture was stirred for 23 h at ambient temperature and filtered subsequently. The filter cake was washed with *n*-hexane (2 × 3 mL). The combined filtrates were evaporated to dryness. Final purification was achieved by short-path distillation at $5 \cdot 10^{-3}$ mbar by means of a flame followed by crystallization from a mixture of dichloromethane (120 mL) and *n*-hexane (24 mL) to give a colourless solid **19**. Yield: 0.19 g (12 %). Found: C, 66.17; H, 5.46; N, 8.20 %; $C_{38}H_{38}B_{12}H_4$ requires C, 67.07; H, 5.63; N, 8.23 %; ^{1}H NMR ($CDCl_3$): δ [ppm] = 1.1 - 2.6 (m, br, 10 H, BH), 6.42 (m, 4 H, H4´,7´), 6.89 (m, 4 H, H5´,6´), 7.16 (d, ^3J = 6.3 Hz, 8 H, H_{ortho}), 7.46 (m, 12 H, H_{meta}, H_{para}); ^{1}H{^{11}B} NMR ($CDCl_3$): δ [ppm] = 1.76 (s, 6 H, BH), 2.14 (s, 4 H, BH); ^{13}C{^{1}H} NMR ($CDCl_3$): δ [ppm] = 62.0 (br s, C1), 110.8 (s, C4´,7´), 120.6 (s, C5´,6´), 127.9 (s, C_{para}), 129.3 (s, C_{meta}), 130.0 (s, C_{ortho}), 138.3 (s, C8´,9´), 139.9 (s, C_{ipso}); ^{11}B{^{1}H} NMR ($CDCl_3$): δ [ppm] = –12.8 (2 B), –9.9 (4 B, B4,6,8,11), –8.8 (2 B), –1.8 (2 B), 23.8 (2 B, B2',2''); MS (EI): m/z = 680.4 (M^+), 340.2 (M^{2+}).

1,12-Bis-(1´,3´-diethyl-1´,3´,2´-benzodiazaborol-2´-yl)-1,12-dicarbadodecaborane (20): 2-Bromo-1,3-diethyl-1,3,2-benzodiazaborole (0.66 g, 2.61 mmol) was added to a slurry of 1,12-dilithio-1,12-dicarbadodecaborane, prepared from 1,12-dicarbadodecaborane (0.17 g, 1.18 mmol) and a *tert*-butyllithium solution (1.7 M in *n*-hexane, 1.55 mL, 2.64 mmol) in boiling *n*-hexane (6 mL) for 2 h. The mixture was heated two further hours at reflux temperature, diluted with an *n*-hexane (5 mL) and filtered subsequently. The filter cake was washed with *n*-hexane (5 mL) and the filtrates were freed from volatile compounds *in vacuo*. Purification of the crude product was achieved by short-path distillation at $5 \cdot 10^{-3}$ mbar followed by crystallization from a mixture of dichloromethane (36 mL) and *n*-hexane (12 mL). Thereby colourless solid **20** was obtained. Yield: 0.09 g (16 %). Found: C, 53.69; H, 7.81; N, 11.47 %; $C_{22}H_{38}B_{12}N_4$ requires C, 54.11; H, 7.84; N, 11.47 %; ^{1}H NMR ($CDCl_3$): δ [ppm] = 1.29 (t, ^3J = 6.9 Hz, 12 H, CH_3), 2.0 - 3.5 (m, br, 10 H, BH), 3.91 (q, ^3J = 6.9 Hz, 8

H, CH_2), 7.03 (m, 8 H, H4´,5´,6´,7´); $^1H\{^{11}B\}$ NMR ($CDCl_3$): δ [ppm] = 2.70 (s, 10 H, BH); $^{13}C\{^1H\}$ NMR ($CDCl_3$): δ [ppm] = 15.9 (s, CH_3), 37.7 (s, CH_2), 109.4 (s, C4´,7´), 119.7 (s, C5´,6´), 136.5 (s, C8´,9´), The resonance of C1 was covered by the solvent signal. It was calculated at 79.9 ppm; $^{11}B\{^1H\}$ NMR ($CDCl_3$): δ [ppm] = –10.9 (10 B, B2-11), 23.7 (2 B, B2',2"); MS (EI): m/z = 488.4 (M^+), 471.3 (M^+-CH_3), 244.2 (M^{2+}).

1,12-Bis-(1´,3´-diphenyl-1´,3´,2´-benzodiazaborol-2´-yl)-1,12-dicarbadodecaborane (21): A solution of 2-bromo-1,3-diphenyl-1,3,2-benzodiazaborole (1.65 g, 4.74 mmol) in benzene (10 mL) was added to a slurry of 1,12-dilithio-1,12-dicarbadodecaborane, prepared from 1,12-dicarbadodecaborane (0.31 g, 2.15 mmol) and a *tert*-butyllithium solution (1.6 M in *n*-hexane, 2.95 mL, 4.72 mmol) by boiling for 2 h in *n*-hexane (12 mL). The mixture was heated for another 3 h at reflux temperature and filtered subsequently. The filter cake was washed with *n*-hexane (25 mL), and the collected filtrates were freed from volatiles *in vacuo*. Purification of the residue was achieved by short-path distillation at $3 \cdot 10^{-3}$ mbar followed by crystallization at –20 °C from dichloromethane (50 mL), to afford colourless crystals **21**. Yield: 0.13 g (8 %). Found: C, 60.95; H, 5.32; N, 7.32 %; $C_{38}H_{38}B_{12}H_4 \cdot CH_2Cl_2$ requires C, 61.20; H, 5.27; N, 7.32 %; ^1H NMR ($CDCl_3$): δ [ppm] = 1.2 - 2.5 (m, br, 10 H, BH), 6.35 (m, 4 H, H4´,7´), 6.83 (m, 4 H, H6´,7´), 7.14 (dd, ^3J = 7.5 Hz, ^4J = 1.9 Hz, 8 H, H_{ortho}), 7.42 (m, 12 H, H_{meta}, H_{para}); $^1H\{^{11}B\}$ NMR ($CDCl_3$): δ [ppm] = 1.84 (s, 10 H, BH); $^{13}C\{^1H\}$ NMR ($CDCl_3$): δ [ppm] = 75.5 (br s, C1), 110.7 (s, C4´,7´), 120.4 (s, C5´,6´), 127.7 (s, C_{para}), 129.2 (s, C_{meta}), 129.9 (s, C_{ortho}), 138.3 (s, C8´,9´), 140.0 (s, C_{ipso}); $^{11}B\{^1H\}$ NMR ($CDCl_3$): δ [ppm] = –11.7 (10 B, B2-11), 23.7 (2 B, B2',2"); MS (EI): m/z = 680.4 (M^+), 340.2 (M^{2+}).

2-*tert*-Butyl-1,3-diethyl-1,3,2-benzodiazaborole (22): An equimolar amount of *tert*-butyllithium solution (1.6 M in *n*-pentane, 2.00 mL, 3.20 mmol) was added dropwise to a solution of 2-bromo-1,3-diethyl-1,3,2-benzodiazaborole (0.81 g, 3.20 mmol) in *n*-pentane (30 mL). After 45 minutes stirring at ambient temperature the mixture was filtered and the filtrate was freed from volatiles *in vacuo*. 2-*tert*-Butyl-1,3-diethyl-1,3,2-benzodiazaborole **22** was obtained as a colourless solid. Yield: 0.53 g (72 %). Further purification was achieved by recrystallisation from *n*-pentane. Found: C, 73.09; H, 10.55; N, 12.23 %; $C_{14}H_{23}BN_2$ requires C, 73.06; H, 10.07; N, 12.17 %; ^1H NMR (C_6D_6): δ [ppm] = 1.07 (t, $^3J_{H,H}$ = 7.1Hz, 6 H, $NCH_2C\underline{H}_3$), 1.22 (s, 9 H, $C(CH_3)_3$), 3.65 (q, $^3J_{H,H}$ = 7.1Hz, 4 H, $NC\underline{H}_2CH_3$), 6.91 (m, 2 H, H4,7), 7.11 (m, 2 H, H5,6); $^{13}C\{^1H\}$ NMR (C_6D_6): δ [ppm] = 15.6 (s, $NCH_2\underline{C}H_3$), 29.9 (s,

C($\underline{C}H_3)_3$), 37.6 (s, N$\underline{C}H_2CH_3$), 108.3 (s, C4,7), 118.7 (s, C5,6), 137.6 (s, C8,9); the $\underline{C}CH_3$ peak was not observed – calculated at 21.6 ppm; $^{11}B\{^1H\}$ NMR (C_6D_6): δ [ppm] = 30.5 (s); MS (EI): m/z = 230.2 (M^+), 215.1 (M^+-Me), 201.1 (M^+-Et).

2-*tert*-Butyl-1,3-diphenyl-1,3,2-benzodiazaborole (23): A *tert*-butyllithium solution (1.6 M in *n*-pentane, 1.40 mL, 2.24 mmol) was added dropwise to a solution of 2-bromo-1,3-diphenyl-1,3,2-benzodiazaborole (0.71 g, 2.02 mmol) in benzene (4.5 mL). After stirring for 1 h the mixture was filtered and the filter-cake was extracted with *n*-pentane (5 mL). The combined filtrates were freed from volatile materials *in vacuo* and the remainder was purified by short-path distillation at $5 \cdot 10^{-3}$ mbar by means of a flame. The sublimate was taken up in a mixture of dichloromethane (5 mL) and *n*-hexane (6 mL) and the resulting solution was concentrated *in vacuo* until the onset of precipitation. Colourless crystals of **23** were grown from this mixture at –30 °C. Yield: 0.23 g (35 %). Found: C, 80.73; H, 7.11; N, 8.55 %; $C_{22}H_{23}BN_2$ requires C, 80.99; H, 7.11; N, 8.59 %; ^1H NMR ($CDCl_3$): δ [ppm] = 0.90 (s, 9 H, C($CH_3)_3$), 6.56 (m, 2 H, H4,7), 6.88 (m, 2 H, H5,6), 7.36 (d, $^3J_{HH}$ = 5.0 Hz, 4 H, H_{ortho}), 7.40 (t, $^3J_{HH}$ = 7.5 Hz, 2 H, H_{para}), 7.49 (dd, $^3J_{HH}$ = 7.5 Hz, $^3J_{HH}$ = 5.0 Hz, 4 H, H_{meta}); $^{13}C\{^1H\}$ NMR ($CDCl_3$): δ [ppm] = 30.4 (s, C($\underline{C}H_3)_3$), 109.8 (s, C4,7), 119.4 (s, C5,6), 127.2 (s, C_{para}), 129.3 (s, C_{meta}), 129.5 (s, C_{ortho}), 139.1 (s, C8,9), 142.1 (s, C_{ipso}), the $\underline{C}CH_3$ peak was not observed – calculated at 20.8 ppm; $^{11}B\{^1H\}$ NMR ($CDCl_3$): δ [ppm] = 31.4 (s); MS (EI): m/z = 326.2 (M^+), 311.1 (M^+–Me).

Photophysical measurements

For all solution state measurements, samples were placed in quartz cuvettes of 10 × 10 mm (Hellma type 111-QS, suprasil, optical precision). Cyclohexane was used as received from commercial sources (p. a. quality), the other solvents were dried by standard methods prior to use. Concentrations varied from 20 to 70 µM according to their optical density. Solid samples were prepared by vacuum sublimation on quartz plates (35 × 10 × 1 mm) using standard Schlenk equipment and conditions. Each plate was placed in a 100 mL round bottom flask and a crystal of the sample, placed underneath it, was sublimed. Absorption was measured with a UV/VIS double-beam spectrometer (Shimadzu UV-2550), using the solvent as a reference.

The output of a continuous Xe-lamp (75 W, LOT Oriel) was wavelength-separated by a first monochromator (Spectra Pro ARC-175, 1800 l/mm grating, Blaze 250 nm) and then used to irradiate a sample. The fluorescence was collected by mirror optics at right angles and imaged

on the entrance slit of a second spectrometer while compensating astigmatism at the same time. The signal was detected by a back-thinned CCD camera (RoperScientific, 1024 \ 256 pixels) in the exit plane of the spectrometer. The resulting images were spatially and spectrally resolved. As the next step, an averaged fluorescence spectrum was calculated from the raw images and stored in the computer. This process was repeated for different excitation wavelengths. The result is a two-dimensional fluorescence pattern with the *y*-axis corresponding to the excitation, and the *x*-axis to the emission wavelength. The wavelength range is λ_{ex} = 230-430 nm (in 1 nm increments) for the UV light and λ_{em} = 305-894 nm for the detector. The time to acquire a complete EES is typically less than 15 min. Post-processing of the EES includes subtraction of the dark current background, conversion of pixel to wavelength scales, and multiplication with a reference file to take the varying lamp intensity as well as grating and detection efficiency into account. The quantum yields were determined against POPOP (*p*-bis-5-phenyl-oxazolyl(2)-benzene) (Φ_F = 0.93) as the standard.

The solid-state fluorescence was measured by addition of an integrating sphere (Labsphere, coated with Spectralon, Ø 12.5 cm) to the existing experimental setup. At the exit slit of the first monochromator the exciting light was transferred into a quartz fiber (LOT Oriel, LLB592). It passed a condensor lens and illuminated a 1 cm^2 area on the sample in the centre of the sphere. The emission and exciting light was imaged by a second quartz fiber on the entrance slit of the detection monochromator. The optics for correction of astigmatism was passed by the light on this way.

Post-processing of the spectra was done as described above. The measurement and calculation of quantum yields was performed according to the method described by Mello.[32] Stokes shifts were calculated from excitation and emission maxima, which were extracted from spectra that were converted from wavelength to wavenumbers beforehand.

Luminescence lifetimes of solid **16** - **21** were measured with a time-correlated single-photon counting apparatus (TCSPC, Horiba Jobin Yvon FluoroHub, light source: Nano-LED280, detector: Photomultiplier TBX).

Electrochemistry

Cyclic voltammetry measurements were carried out using an EcoChemie Autolab PG-STAT 30 potentiostat at 298 K with a platinum or glassy carbon working electrode and platinum

wires as counter and reference electrodes in a nitrogen-containing glove box with 0.1 M $^{n}Bu_4NPF_6$ in dichloromethane or acetonitrile. Scan rates of 100 mV s^{-1} and analyte concentrations of 10^{-3} M were used. The ferrocene/ferrocenium FcH/FcH^+ couple served as internal reference at 0.0 V for potential measurements. Cyclic voltammetry simulations were carried out with the ESP software.[33]

Crystallographic studies

Single crystals were coated with a layer of hydrocarbon oil and attached to a glass fiber. Crystallographic data were collected with a Nonius KappaCCD or a Bruker KAPPA APEX II diffractometer with Mo-Kα radiation (graphite monochromator, λ = 0.71073 Å) at 100 K. Crystallographic programs used for structure solution and refinement were from SHELX-97.[34] The structures were solved by direct methods and were refined by using full-matrix least squares on F^2 of all unique reflections with anisotropic thermal parameters for all non-hydrogen atoms, except disordered atoms in **17**, **19** and **21**. All hydrogen atoms were refined isotropically for **16**, **21** and **23**. For **17**, **18** and **19** only the hydrogen atoms bonded to the carborane unit were refined isotropically, the other hydrogen atoms were refined using a riding model with U(H) = 1.5 U_{eq} for CH_3 groups and U(H) = 1.2 U_{eq} for all others. Crystallographic data for the compounds are listed in Table S1. CCDC-847434 (**16**), CCDC-847435 (**17**), CCDC-847436 (**18**), CCDC-847437 (**19**), CCDC-929985 (**21**) and CCDC-929986 (**23**), contain the supplementary crystallographic data for this paper. These data can be obtained free of charge from the Cambridge Crystallographic Data Centre via www.ccdc.cam.ac.uk/data_request/cif

Computational details

All computations were carried out with the Gaussian 09 package.[35] The model geometries were fully optimized with the B3LYP functional[36] with no symmetry constraints using the 6-31G* basis set[37] for all atoms. Frequency calculations on these optimized geometries (**16-23**) revealed no imaginary frequencies. Computed absorption data were obtained from TD-DFT[38] calculations on S_0 geometries whereas computed emission data were derived from the S_1 geometries. The MO diagrams and MO compositions were generated with the Gabedit[39] and GaussSum[40] packages respectively. Calculated ^{11}B, ^{13}C and ^{1}H NMR chemical shifts obtained at GIAO[41]-B3LYP/6-31G*//B3LYP/6-31G* on the optimized geometries were referenced to $BF_3{\cdot}OEt_2$ for ^{11}B: $\delta(^{11}B) = 111.7 - \sigma(^{11}B)$ and referenced to TMS for ^{13}C: $\delta(^{13}C) = 189.4 -$

$\sigma(^{13}C)$ and ^{1}H: δ (^{1}H) = 32.39 - $\sigma(^{1}H)$. Computed NMR values reported here were averaged where possible.

References

1. L. Duan, J. Qiao, Y. Sun and Y. Qiu, *Adv. Mater*., 2011, **23**, 1137-1144.
2. A. Chaskar, H.-F. Chen and K.-T. Wong, *Adv. Mater*., 2011, **23**, 3876-3895.
3. R. N. Grimes, *Carboranes*, 2nd edition; Academic Press (Elsevier) New York 2011.
4. K.-R. Wee, W.-S. Han, D. W. Cho, S. Kwon, C. Pac and S. O. Kang, *Angew. Chem. Int. Ed.* 2012, **51**, 2677-2680.
5. J. J. Peterson, M. Werre, Y. C. Simon, E. B. Coughlin and K. R. Carter, *Macromolecules* 2009, **42**, 8594-8598.
6. K. Kokado and Y. Chujo, *J. Org. Chem.* 2011, **76**, 316-319.
7. J. J. Peterson, Y. C. Simon, E. B. Coughlin and K. R. Carter, *Chem. Commun*., **2009**, 4950-4952.
8. L. Weber, J. Kahlert, R. Brockhinke, L. Böhling, A. Brockhinke, H.-G. Stammler, B. Neumann, R. A. Harder and M. A. Fox, *Chem. Eur. J.* 2012, **18**, 8347-8357.
9. B.P. Dash, R. Satapathy, E.R. Galliard, K.M. Norton, J.A. Maguire, N. Chug and N.S. Hosmane, *Inorg. Chem.*, 2011, **50**, 5485-5493.
10. K. Kokado, Y. Tokoro and Y. Chujo, *Macromolecules* 2009, **42**, 9238-9242.
11. K. Kokado, Y. Tokoro and Y. Chujo, *Macromolecules* 2009, **42**, 2925-2930.
12. (a) K. Kokado, A. Nagai and Y. Chujo, *Macromolecules* 2010, **43**, 6463-6468; (b) K. Kokado and Y. Chujo, *Macromolecules* 2009, **42**, 1418-1420; (c) K. Kokado, A. Nagai and Y. Chujo, *Tetrahedron Lett.* 2011, **52**, 293-296; (d) J.J. Peterson, A.R. Davis, M. Werre, E.B. Coughlin and K.R. Carter, *ACS Appl. Mater. Interfaces* 2011, **3**, 1796-1799.
13. (a) A. Ferrer-Ugalde, E. J. Juárez-Pérez, F. Teixidor, C. Viñas, R. Sillanpää, E. Pérez-Inestrosa and R. Núñez, *Chem. Eur. J.* 2011, **17**, 544-553; (b) F. Lerouge, A. Ferrer-Ugalde, C. Viñas, F. Teixidor, R. Sillanpää, A. Abreu, E. Xochitiotzi, N. Farfán, R. Santillan and R. Núñez, *Dalton Trans.*, 2011, **40**, 7541-7550; (c) F. Lerouge, C. Viñas, F. Teixidor, R. Núñez, A. Abreu, E. Xochitiotzi, R. Santillan and N. Farfán, *Dalton Trans.*, **2007**, 1898-1903; (d) K.C. Song, H. Kim, K.M. Lee, Y.S. Lee, Y. Do and M.H. Lee, *Dalton Trans.*, 2013, **42**, 2351-2354.

14. (a) B. Le Guennic, K. Costuas, J.F. Halet, C. Nervi, M.A.J. Paterson, M.A. Fox, R.L. Roberts, D. Albesa-Jove, H. Puschmann, J.A.K. Howard and P.J. Low, *Comptes Rendus Chimie*, 2005, **8**, 1883-1896; (b) L. Drož, M.A. Fox, D. Hnyk, P.J. Low, J.A.H. MacBride and V. Všetečka, *Coll. Czech. Chem. Commun*., 2009, **74**, 131-146.

15. (a) L. A. Boyd, W. Clegg, R. C. B. Copley, M. G. Davidson, M. A. Fox, T. G. Hibbert, J. A. K. Howard, A. Mackinnon, R. J. Peace and K. Wade, *Dalton Trans*. **2004**, 2786-2799; (b) J. M. Oliva, N. L. Allan, P. v. R. Schleyer, C. Viñas and F. Teixidor, *J. Am. Chem. Soc*. 2005, **127**, 13538-13547; (c) B. W. Hutton, F. MacIntosh, D. Ellis, F. Herisse, S. A. Macgregor, D. McKay, V. Petrie-Armstrong, G. M. Rosair, D. S. Perekalin, H. Tricas and A. J. Welch, *Chem. Commun*. **2008**, 5345-5347; (d) M. A. Fox, J. A. H. MacBride, R. J. Peace, W. Clegg, M. R. J. Elsegood and K. Wade, *Polyhedron* 2009, **28**, 789-795; (e) M. A. Fox, R. J. Peace, W. Clegg, M. R. J. Elsegood and K. Wade, *Polyhedron* 2009, **28**, 2359-2370.

16. M. A. Fox, C. Nervi, A. Crivello and P. J. Low, *Chem. Commun.* **2007**, 2372-2374.

17. L. Weber, J. Kahlert, L. Böhling, A. Brockhinke, H.-G. Stammler, B. Neumann, R. A. Harder, P.J. Low and M. A. Fox, *Dalton Trans.* 2013, **42**, 2266-2281.

18. A. R. Davis, J.J. Peterson and K. R. Carter, *ACS Macro Lett.*, 2012, **1**, 469-472.

19. K.R. Wee, Y.J. Cho, S. Jeong, S. Kwon, J.D. Lee, I.H. Suh and S.O. Kang, *J. Am. Chem. Soc.*, 2012, **134**, 17982-17990.

20. (a) L. Weber, I. Domke, C. Schmidt, T. Braun, H.-G. Stammler and B. Neumann, *Dalton Trans.* **2006**, 2127-2132; (b) L. Weber, V. Werner, M. A. Fox, T. B. Marder, S. Schwedler, A. Brockhinke, H.-G. Stammler and B. Neumann, *Dalton Trans*. **2009**, 1339-1351; (c) S. Schwedler, D. Eickhoff, R. Brockhinke, D. Cherian, L. Weber and A. Brockhinke, *Phys. Chem. Chem. Phys.* 2011, **13**, 9301-9310; (d) L. Weber, D. Eickhoff, V. Werner, L. Böhling, S. Schwedler, A. Chrostowska, A. Dargelos, M. Maciejczyk, H.-G. Stammler and B. Neumann, *Dalton Trans.* 2011, **40**, 4434-4446; (e) L. Weber, D. Eickhoff, J. Kahlert, L. Böhling, A. Brockhinke, H.-G. Stammler, B. Neumann and M. A. Fox, *Dalton Trans.* 2012, **41**, 10328-10346; (f) L. Weber, H. Kuhtz, L. Böhling, A. Brockhinke, A. Chrostowska, A. Dargelos, A. Mazière, H.-G. Stammler and B. Neumann, *Dalton Trans.* 2012, **41**, 10328-10346; (g) L. Weber, D. Eickhoff, T. B. Marder, M. A. Fox, P. J. Low, A. D. Dwyer, D. J. Tozer, S. Schwedler, A. Brockhinke, H.-G. Stammler and B. Neumann, *Chem. Eur. J.* 2012, **18**, 1369-1382.

21. (a) L. Weber, A. Penner, I. Domke, H.-G. Stammler and B. Neumann, *Z. Anorg. Allg. Chem.* 2007, **633**, 563-569; (b) L. Weber, V. Werner, I. Domke, H.-G. Stammler and B. Neumann, *Dalton Trans.* **2006**, 3777-3784; (c) S. Maruyama and Y. Kawanishi, *J. Mater. Chem.* 2002, **12**, 2245-2249.

22. L. Weber, V. Werner, M. A. Fox, T. B. Marder, S. Schwedler, A. Brockhinke, H.-G. Stammler and B. Neumann, *Dalton Trans.* **2009**, 2823-2831.

23. L. Weber, J. Halama, V. Werner, K. Hanke, L. Böhling, A. Chrostowska, A. Dargelos, M. Maciejczyk, A. L. Raza, H.-G. Stammler and B. Neumann, *Eur. J. Inorg. Chem.* **2010**, 5416-5425.

24. (a) C.A. Slabber, C.D. Grimmer and R.S. Robinson, *J. Organomet. Chem.*, 2013, **723**, 122-128; (b) R.S. Robinson, S. Sithebe and M.P. Akerman, *Acta Cryst.*, 2012, **E68**, o2241-o2241; (c) N. Maraš and M. Kočevar, *Helv. Chim. Acta*, 2011, **94**, 1860-1874; (d) T. Kojima, D. Kumaki, J. Nishida, S. Tokito and Y. Yamashita, *J. Mater. Chem.*, 2011, **21**, 6607-6613.

25. Patent Merck GmbH, Darmstadt, Germany WO2010/099852A1, 2010.

26. (a) S. Hayashi and T. Koizumi, *Polym. Chem.*, 2012, **3**, 613-616; I. Yamaguchi, T. Tominaga and M. Sato, *Polym. Int.*, 2009, **58**, 17-21; (b) I. Yamaguchi, B.-J. Choi, T. Koizumi, K. Kubota and T. Yamamoto, *Macromolecules*, 2007, **40**, 438-443; (c) H. Kuhtz, F. Cheng, S. Schwedler, L. Böhling, A. Brockhinke, L. Weber, K. Parab and F. Jäkle, *ACS Macro Lett.*, 2012, **1**, 555-559.

27. (a) G. Zi, H.-W. Li and Z. Xie, *Organometallics*, 2002, **21**, 1136-1145; (b) Y.Z. Voloshin, S.Y. Erdyakov, I.G. Makarenko, E.G. Lebed', T.V. Potapova, S.V. Svidlov, Z.A. Starikova, E.V. Pol'shin, M.E. Gurskii and Y.N. Bubnov, *Russ. Chem. Bull., Int. Ed.*, 2007, **56**, 1787-1794; (c) S.Y. Erdyakov, Y.Z. Voloshin, I.G. Makarenko, E.G. Lebed, T.V. Potapova, A.V. Ignatenko, A.V. Vologzhanina, M.E. Gurskii and Y.N. Bubnov, *Inorg. Chem. Commun.*, 2009, **12**, 135-139; (d) G. Zi, H.-W. Li and Z. Xie, *Organometallics*, 2002, **21**, 3850-3855.

28. M. A. Fox, C. Nervi, A. Crivello, A. S. Batsanov, J. A. K. Howard, K. Wade and P. J. Low, *J. Solid State Electrochem.* 2009, **13**, 1483-1495.

29. (a) H. Tricas, M. Colon, D. Ellis, S. A. Macgregor, D. McKay, G. M. Rosair, A. J. Welch, I. V. Glukhov, F. Rossi, F. Laschi and P. Zanello, *Dalton Trans.* 2011,**40**, 4200-4211; (b) K. Hosoi, S. Inagi, T. Kubo and T. Fuchigami, *Chem. Commun.* 2011, **47**, 8632-8634.

30. P. Zanello, C. Nervi and F. Fabrizi de Biani, *Inorganic Electrochemistry. Theory, Practice and Application*, 2nd Ed., RSC, 2011.

31. L. Weber, H. B. Wartig, H.-G. Stammler and B. Neumann, *Z. Anorg. Allg. Chem.* 2001, **627**, 2663-2668.

32. J. C. de Mello, H. F. Wittmann and R. H. Friend, *Adv. Mater.* 1997, **9**, 230-232.

33. ESP (Electrochemical Simulation Package); http://lem.ch.unito.it/esp_manual.html

34. G. M. Sheldrick, *Acta Cryst*. 2008, **A64**, 112-122.

35. Gaussian 09, Revision A.02, M. J. Frisch, G. W. Trucks, H. B. Schlegel, G. E. Scuseria, M. A. Robb, J. R. Cheeseman, G. Scalmani, V. Barone, B. Mennucci, G. A. Petersson, H. Nakatsuji, M. Caricato, X. Li, H. P. Hratchian, A. F. Izmaylov, J. Bloino, G. Zheng, J. L. Sonnenberg, M. Hada, M. Ehara, K. Toyota, R. Fukuda, J. Hasegawa, M. Ishida, T. Nakajima, Y. Honda, O. Kitao, H. Nakai, T. Vreven, Jr., J. A. Montgomery, J. E. Peralta, F. Ogliaro, M. Bearpark, J. J. Heyd, E. Brothers, K. N. Kudin, V. N. Staroverov, R. Kobayashi, J. Normand, K. Raghavachari, A. Rendell, J. C. Burant, S. S. Iyengar, J. Tomasi, M. Cossi, N. Rega, J. M. Millam, M. Klene, J. E. Knox, J. B. Cross, V. Bakken, C. Adamo, J. Jaramillo, R. Gomperts, R. E. Stratmann, O. Yazyev, A. J. Austin, R. Cammi, C. Pomelli, J. W. Ochterski, R. L. Martin, K. Morokuma, V. G. Zakrzewski, G. A. Voth, P. Salvador, J. J. Dannenberg, S. Dapprich, A. D. Daniels, O. Farkas, J. B. Foresman, J. V. Ortiz, J. Cioslowski and D. J. Fox, *Gaussian, Inc.*, Wallingford CT, **2009**.

36. (a) A. D. Becke, *J. Chem. Phys.* 1993, **98**, 5648-5652; (b) C. Lee, W. Yang and R. G. Parr, *Phys. Rev. B* 1988, **37**, 785-789.

37. (a) G. A. Petersson and M. A. Al-Laham, *J. Chem. Phys.* 1991, **94**, 6081-6090; (b) G. A. Petersson, A. Bennett, T. G. Tensfeldt, M. A. Al-Laham, W. A. Shirley and J. Mantzaris, *J. Chem. Phys.* 1988, **89**, 2193-2218.

38. E. Runge and E. K. U. Gross, *Phys. Rev. Lett.* 1984, **52**, 997-1000.

39. A. R. Allouche, *J. Comp. Chem.* 2011, **32**, 174-182.

40. N. M. O'Boyle, A. L. Tenderholt, K. M. Langner, *J. Comp. Chem*. 2008, **29**, 839-845.

41. (a) R. Ditchfield, *Mol. Phys.* 1974, **27**, 789-807; (b) C.M. Rohling, L.C. Allen and R. Ditchfield, *Chem. Phys.* 1984, **87**, 9-15; (c) K. Wolinski, J. F. Hinton and P. Pulay, *J. Am. Chem. Soc*. 1990, **112**, 8251-8260.